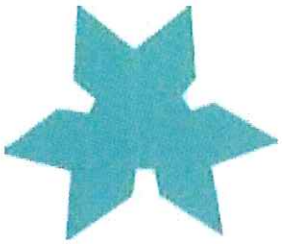

# FORTH AND TAY OFFSHORE WIND DEVELOPERS GROUP: CETACEAN SURVEY DATA ANALYSIS REPORT

PREPARED FOR SMRU LIMITED

18 June 2012

DMP STATS

DMP STATS The Coach House, Mount Melville House, St. Andrews, Scotland KY 168 NT, UK +44(0) 1334 477 544 mail@dmpstats.com

| REPORT INFORMATION | | | |
|---|---|---|---|
| CURRENT DOCUMENT | | | |
| Version | Issued Date | Author(s) | Status |
| 1.3 | 18/06/2012 | [Redacted] | Final version |
| REVISION HISTORY | | | |
| Version | Issued Date | Author(s) | Status |
| 1.0 | 30/05/2012 | [Redacted] | Draft |
| 1.1 | 30/05/2012 | | Final version |
| 1.2 | 11/06/2012 | | Final version |

DMP STATS The Coach House, Mount Melville House, St. Andrews, Scotland KY 168 NT, UK +44(0) 1334 477 544 mail@dmpstats.com

## CONTENTS

DMP STATS The Coach House, Mount Melville House, St. Andrews, Scotland KY 168 NT, UK +44(0) 1334 477 544 mail@dmpstats.com

# 1 OVERVIEW

This document presents the results of statistical analyses of survey data for the Forth and Tay Offshore Wind Developers Group (FTOWDG hereafter) survey area. We first present a description of the methods, followed by the results of the analyses. The analysis outputs mainly consist of spatial surfaces with associated estimates of abundances for harbour porpoises, white-beaked dolphins and minke whales (across the survey period) and inference about both the surface and abundance estimates. As such, the bulk of deliverables are the report's graphics and their associated datasets, which are supplementary to this report.

# 2 ACTIVITIES

SMRU Limited requested from DMP Statistical Solutions UK Limited (DMP hereafter), a package of outputs that reflect the spatial distribution of three species/groups through time. The outputs were to be mainly graphical, comprising of relative/absolute density surfaces & associated inference.

The following analysis activities were carried out to meet SMRU Limited's requests.

## 2.1 DATA PREPARATION, CALCULATION OF SURVEY EFFORT

The preliminary data management phase, for the boat and aerial survey data required:

i. Combining of all data sources into file(s) amenable to statistical analysis.

ii. Checking and correcting for erroneous values, condensing of detail unnecessary for the plotting and modelling.

iii. Determining survey effort from transect characteristics.

iv. Setting and summarising to an appropriate spatio-temporal resolution.

v. Expansion of data to include survey points where animals were not observed.

vi. Quality assurance: iterations of data checking/plots, querying client and subsequent modification.

## 2.2 ESTIMATING ABUNDANCES ALONG THE TRANSECT LINES

The raw/observed counts were inflated using distance sampling analysis[1] to account for imperfect detection from the plane or boat (section 3) and since the animals under study are very often underwater (and therefore unavailable to be seen from the plane or boat), this analysis also involved a correction for availability (section 4.4), when calculating estimates of abundance.

## 2.3 DENSITY SURFACE FITTING

The corrected counts for imperfect detection for each segment were used as inputs for the statistical models in order to produce species distribution maps for the three species. The details of the modelling process are given in Section 3. Uncertainties were quantified for all of these outputs and relative and absolute abundances calculated for each species (Section 4.2) with associated 95% confidence intervals.

## 2.4 OUTPUTS

The main output for this work is this report, however the data underpinning the majority of plots have also been provided in CSV format.

[1] Thomas, L., S.T. Buckland, E.A. Rexstad, J. L. Laake, S. Strindberg, S. L. Hedley, J. R.B. Bishop, T. A. Marques, and K. P. Burnham. 2010. Distance software: design and analysis of distance sampling surveys for estimating population size. Journal of Applied Ecology 47: 5-14. DOI: 10.1111/j.1365-2664.2009.01737.x

DMP STATS The Coach House, Mount Melville House, St. Andrews, Scotland KY 168 NT, UK +44(0) 1334 477 544 mail@dmpstats.com

# 3 ESTIMATING ABUNDANCE USING DISTANCE SAMPLING ANALYSIS

## 3.1 DATA ISSUES

For the aerial data set, individual lines were identified using the date, transect number and direction of travel. The total effort for each line was calculated using start/stop coordinates for port and starboard (i.e. 'seat') observer effort. Observations were also matched to lines using time, date, transect number and seat information.

For the Firth of Forth data set, perpendicular distances were calculated for each observation using bearing from observer, line orientation and distance from observer. Observations were also matched to lines using time, date, route, line and survey data. 19 observations did not match any of the lines and were therefore not included in the analysis. 14 further observations could also not be allocated to segments; 3 of these were due to the recorded spatial co-ordinates for these observations being too far from the line and 11 were due to incorrect spatial co-ordinates for lines 20_8_2_P2 and 23_8_2_P2.

## 3.2 DETECTION FUNCTION MODEL SELECTION

Half-normal and hazard-rate models were compared for each data set, using the available covariates associated with the observation data in each case to construct the candidate models. Summary information on the chosen models for each data set for harbour porpoises is given in Table 1.

| | Number of detected groups (hp) | Distances collected in bins | Additional right truncation | Detection function used | $X^2$ GOF test p-value |
|---|---|---|---|---|---|
| Aerial | 228 | Yes | - | Hazard rate (no covariates) | * |
| FoF | 107 | No | 400m | Hazard rate (no covariates) | 0.9363 |
| Inch Cape | 57 | No | - | Hazard rate (no covariates) | 0.2917 |
| NnG | 106 | Yes | - | Half normal (no covariates) | 0.3864 |

Table 1: Summary information for fitted detection functions for harbour porpoises. * Too few degrees of freedom were available to carry out this test.

| | Number of detected groups (hp) | Distances collected in bins | Detection function used | $X^2$ GOF test p-value |
|---|---|---|---|---|
| Aerial | 8 | Yes | Half normal (no covariates) | 0.22015 |
| FoF | 56 | No | Hazard rate (no covariates) | 0.40825 |
| Inch Cape | 23 | No | Hazard rate (no covariates) | 0.071251 |
| NnG | 14 | Yes | Half normal (no covariates) | 0.59363 |

Table 2: Summary information for fitted detection functions for Minke Whale

DMP STATS The Coach House, Mount Melville House, St. Andrews, Scotland KY 168 NT, UK +44(0) 1334 477 544 mail@dmpstats.com

| | Number of detected groups (hp) | Distances collected in bins | Detection function used | $X^2$ GOF test p-value |
|---|---|---|---|---|
| Aerial | 63 | Yes | Half normal (no covariates) | 0.2615 |
| FoF | 67 | No | Hazard rate (no covariates) | 0.76494 |
| Inch Cape | 3 | No | Half normal (no covariates) | * |
| NnG | 6 | Yes | Half normal (no covariates) | 0.85895 |

Table 3: Summary information for fitted detection functions for White-beaked Dolphin. * indicates too few degrees of freedom for test

Note:

- Approximately 15% of bootstrap samples for Inchcape minke whale had to be discarded due to model fitting problems.
- Sample sizes for minke whale for Aerial and Nng too small for detection functions or bootstrap to be reliable.
- Sample sizes for white-beaked dolphin for Inchcape and Nng too small for detection functions or bootstrap to be reliable.

## 3.3 SEGMENTATION

Lines from all surveys were divided into 2km by 2km adjoining segments. Observations were assigned to individual segments and individual abundance estimates were obtained for each segment using the fitted detection functions.

## 3.4 DETECTION FUNCTION INFERENCE

To assist the inference process, 500 bootstrap resamples of the detection functions were also produced by resampling lines (with replacement) from each survey. As a part of this process, the preferred detection functions were refitted using the observations from the bootstrap replicates and individual abundance estimates obtained for each segment, in each case. This gave rise to 500 sets of abundance estimates per segment for input to the combined inference process at a later stage (this process is described on page 18).

### 3.4.1 Harbour porpoise detection functions

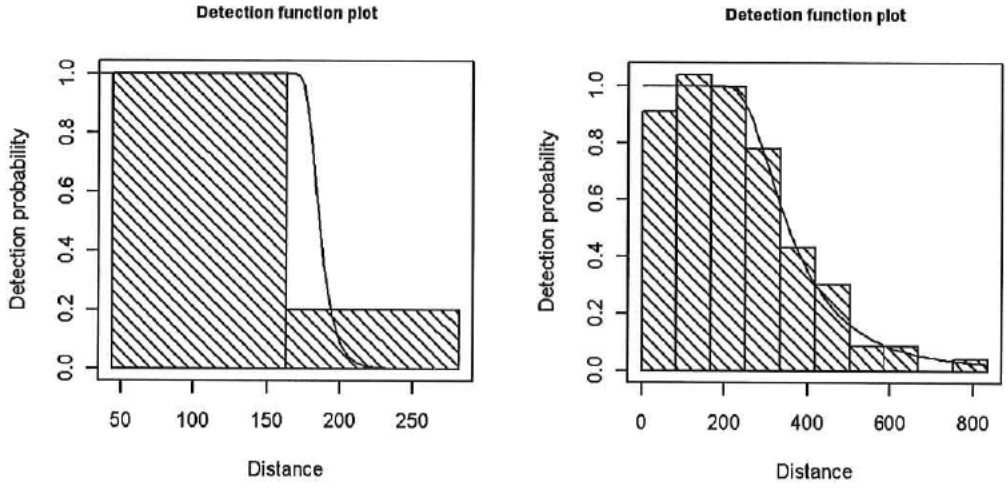


Figure 1 : Fitted detection functions for the aerial survey (left) and Firth of Forth data sets (right).

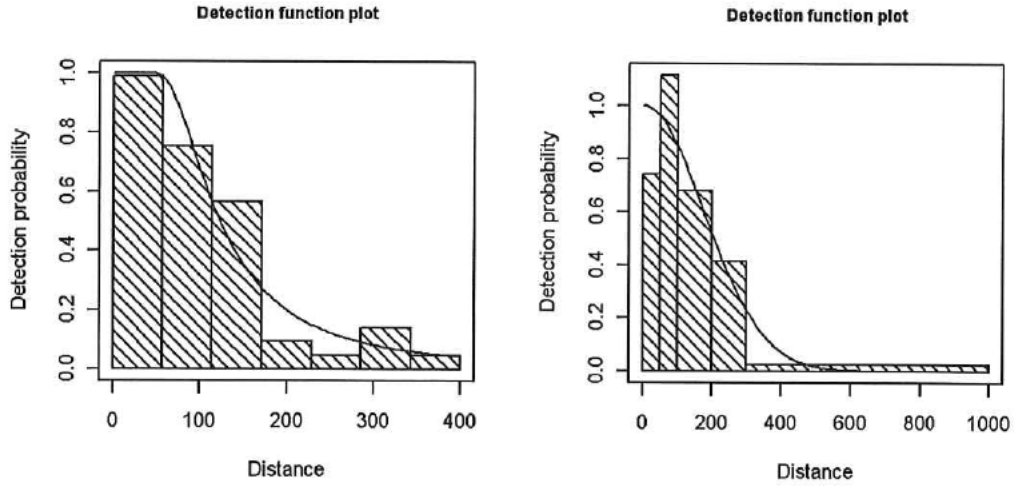


Figure 2 : Fitted detection functions for the Inchcape (left) and NnG (right) data sets.

DMP STATS The Coach House, Mount Melville House, St Andrews, Scotland KY 168 NT, UK +44(0) 1334 477 544 mail@dmpstats.com

### 3.4.2 Minke whale detection functions

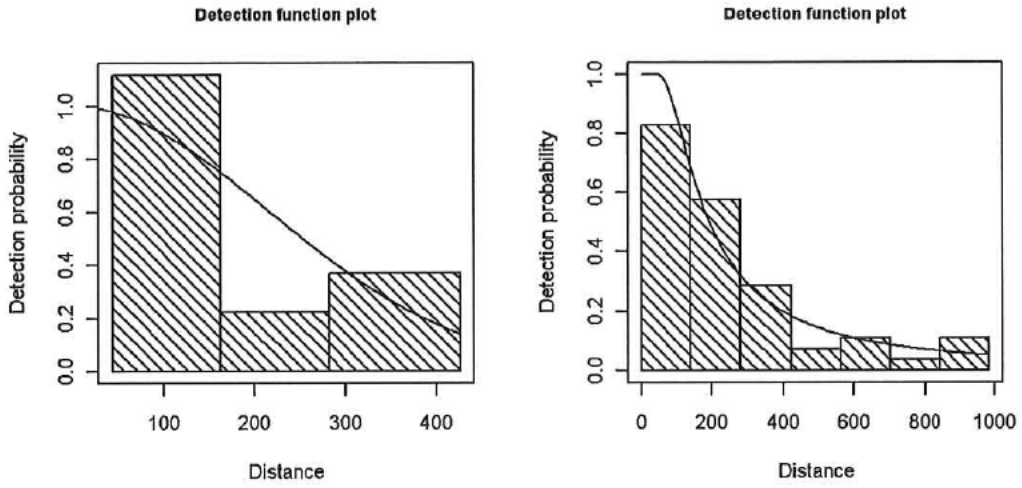


Figure 3: Fitted detection functions for the aerial survey (left) and Firth of Forth data sets (right).

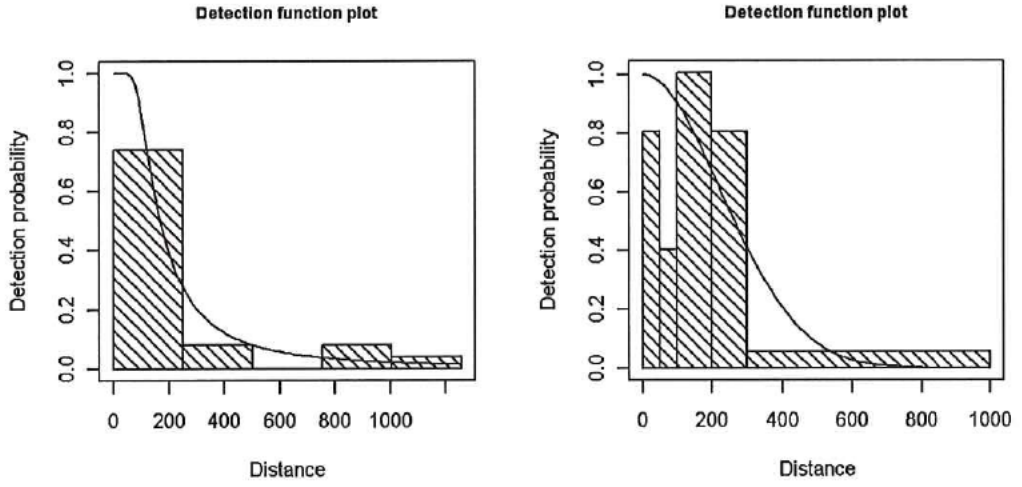


Figure 4: Fitted detection functions for the Inchcape (left) and NnG (right) data sets.

### 3.4.3 White-beaked dolphin detection functions

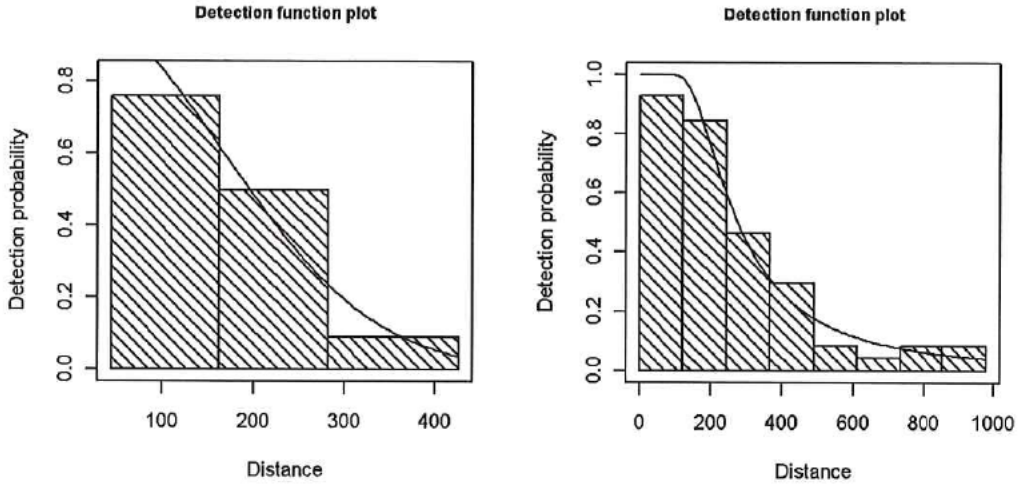


Figure 5: Fitted detection functions for the aerial survey (left) and Firth of Forth data sets (right).

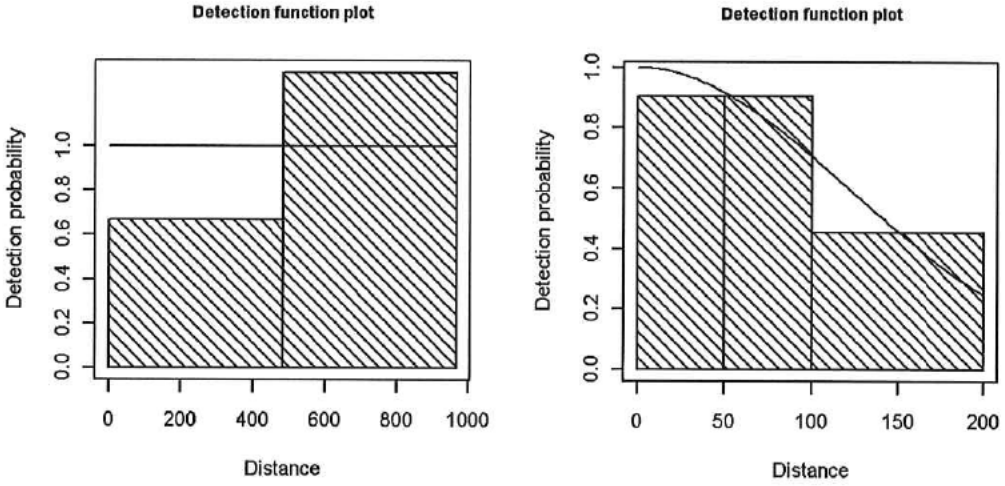


Figure 6: Fitted detection functions for the Inchcape (left) and NnG (right) data sets.

# 4 DENSITY SURFACE FITTING METHODOLOGY

We present here a technical description of the statistical models used to generate the species density maps and abundance estimates. This pre-supposes knowledge of Generalized Linear Models (GLMs) and smoothing methods.

## 4.1 MODEL STRUCTURE

To accommodate local surface features in species distribution and potentially patchy numbers of animals across the survey area, a range of candidate models were considered for the species-specific density surfaces. The scope of the models considered was chosen to adequately capture surfaces with both local surface features (e.g. patchy surfaces with locally acting hotspots) and global surface features (e.g. flat surfaces or far-reaching trends).

The count data were assumed to be (potentially overdispersed) Poisson counts with spatio-temporal autocorrelation. Flexible surfaces were implemented where possible for each species and, data permitting, the surfaces were allowed to change substantially across years (via an interaction effect with the spatial smooth). Month and year were also fitted in each model, where possible, and a log link and overdispersed Poisson errors were assumed for all models. Additionally, while distance sampling methods were used to account for imperfect detection in each survey (see section 3), a 'survey' factor variable was also fitted to describe any overall differences in average numbers across survey type, where they exist. The survey variable comprised of: Forth of Firth (fof), The Crown Estates aerial survey (aerial), Inchcape (Inchcape), and NnG (nng). In short, there may be survey specific differences in animal observations beyond their different detection properties, which will be estimated in the model.

For the two data-sparse species (minke whale and white-beaked dolphin), a low dimensional smooth function was fitted along with year as a factor. This specification necessarily results in spatial surfaces which are very smooth, potentially increasing or decreasing each year across the grid, but not allowing for changes in the spatial distribution across time. 'Month' was excluded from these models due to uniformly zero counts in some months for these species. As for harbour porpoise, 'survey' factor variable was also tested for inclusion in the models.

### 4.1.1 Knot placement and basis function details

Model flexibility for the spatial surfaces in this setting is determined by both the number of 'knots' used (i.e. anchor points) for the model and the effective range ($r$) of the basis associated with each knot. Here $r$ controls the spatial extent to which each knot/basis influences the fitted surface. Since the optimal choices for both of these features are always unknown, these details were considered as a part of the model selection process governed by objective fit criteria.

For a given knot number, the initial knot locations on the spatial surface were chosen to maximise the coverage across the spatial area, via a space filling algorithm[2], and these locations were permitted to move according to the Spatially Adaptive Local Smoothing Algorithm (SALSA[3]) model selection method. The local exponential basis function ((exp(-$d/r^2$) with $d$=Euclidean distance[4]) was implemented and was permitted to have variable $r$-values across the surface, which were dictated by the data. A variable number of knot numbers were used for the candidate models[5] and an objective fit criterion (below) was used to choose the best model(s).

The degree of flexibility permitted for the spatial models was determined using Cross-Validation (CV). This 10-fold CV score balances fit to the data with model complexity and is based on evaluating model predictions to data unseen by the model (validation data). The data are randomly split into 10 mutually exclusive sets and while 9 of the 10 sets are used to train the model, the remaining set is used to evaluate these trained model predictions to the validation set. This is repeated until all 10 sets have acted as validation sets and effectively repeatedly simulates model predictions on unseen data[6]. The sum of the squared differences between the observed data in the validation sets and the predictions based on the training data are then found in each case, and the average of these 10 values used to give a CV score. The QICu scores (AIC-style scores for Generalised Estimating Equation -based models) were also retained for each model.

## 4.2 MODEL INFERENCE

### 4.2.1 Parameter uncertainty in the spatial models

The data are collected along transects and consecutive measurements on these transects are closely linked in space and time. Additionally, due to environmental/prey conditions which may be unknown to us, the abundance of marine mammals at any particular location is likely to be more similar for points close together in time compared with points distant in time. Models fitted to the count data attempt to explain animal abundance at any particular location, but the covariate information that describes why animals are found in high/low numbers at particular locations is often missing from the model. This leaves pattern in the noise component – as represented by model residuals. Further, these patterns are likely to be similar along the track lines. This correlation in model residuals along the track lines violates a critical assumption for standard statistical models (such as GLMs/GAMs) which require independence of errors. Further, ignoring this violation can invalidate all model-based estimates of precision (e.g. standard errors, confidence intervals and $p$-

2 1990. Johnson, M.E., Moore, L.M., and Ylvisaker, D. Minimax and maximin distance designs. Journal of Statistical Planning and Inference 26, 131-148.

3 2011. Walker, C., MacKenzie, M. L., Donovan, C. R.,& O'Sullivan, M. SALSA – A Spatially Adaptive Local Smoothing Algorithm.. Journal of Statistical Computation and Simulation. 81, 2.

4 Geodesic distances (as the animal swims, not as the crow flies) could also be considered here, should physical structures which obstruct animal travel be put in place.

[5] 2-35, depending on data sparsity

[6] Hastie, T., Tibshirani, R. & Friedman, J. (2009) *The elements of statistical learning*. 2nd edition. Springer.

values). Further to this, if the incorrect inference is used in model selection, the selected model may not be justified, meaning even point estimates may be poor. Given positive correlation is typical, the models will tend to be over-complicated and statistical significance tends to be attributed to random fluctuations in the data.

For this reason, a modelling framework which incorporates this autocorrelation was used to obtain realistic model-based estimates of precision in this analysis (Generalized Estimating Equations; GEEs[7]). GEEs are designed to explicitly estimate and incorporate residual autocorrelation within the transects. To ensure this extra complexity was required, a runs-test[8] was employed in each case to test for statistically significant levels of spatio-temporal autocorrelation in model residuals along the transects. In the case that statistically significant levels of autocorrelation were found, flights/tracks/survey lines were used to define the panel/blocking structure. In a GEE setting, correlation is permitted within survey lines but independence between these is assumed.

The GEE method adjusts model-based estimates of precision (e.g. 95% confidence intervals) for the autocorrelation observed in the model residuals, via empirical sandwich estimates of variance, to give robust results and realistic model inference. A substantial amount of temporal autocorrelation was evident in model residuals for all species, and this was determined to be statistically significant at the 1% level in all cases.

### 4.2.2 Combining the uncertainty from the detection function and spatial model processes

A non-parametric bootstrap process was used to provide 500 sets of estimated abundances for each transect segment across the surface, based on the parameter uncertainty at the detection function stage. These bootstrap replicates were then used as inputs into the GEE-based flexible spatial model which was refitted each time. The GEE-based standard errors from each model refit were then used to generate a parametric bootstrap replicate from each of these 500 realisations. These provided empirical confidence intervals across the surface. Note, these geo-referenced confidence intervals include the uncertainty in model parameters at the detection function and spatial modelling stage, spatio-temporal autocorrelation and overdispersion.

## 4.3 MODEL PERFORMANCE IN COMPARISON WITH GENERALIZED ADDITIVE MODELS (GAMS)

For comparison with the spatially adaptive results presented here, results based on Generalized Additive Models (GAMs[9]) are also shown for harbour porpoise, minke whale and the white-beaked dolphins. Typically GAMs are not spatially adaptive and do not account for spatio-temporal autocorrelation, however they represent a commonly used method and offer a convenient comparison with the fitted surfaces provided. In contrast, the method used here is spatially adaptive

7 2002. Hardin, J and Hilbe, J. Generalized Estimating Equations. Chapman and Hall, CRC Press.

8 1982. Mendenhall, W. Statistics for Management and Economics, 4th Ed., 801-807, Duxbury Press, Boston

9 2000. Wood, S.N. Modelling and Smoothing Parameter Estimation with Multiple Quadratic Penalties. J.R.Statist.Soc.B 62(2):413-428

in allocating varying amounts of smoothness across the surface and does account for spatio-temporal autocorrelation. These results are presented in Section 0.

### 4.4 CORRECTING FOR AVAILABILITY

The species under consideration here are most often underwater and are therefore typically unavailable to be seen at the surface. This must be accounted for when estimating absolute animal abundances. The availability of each animal species to be seen at the surface was incorporated by inflating the fitted surfaces by an availability correction, e.g. if animals were available to be seen only 8.8% of the time, then an abundance estimate for the survey area of say 10 animals was inflated to be 10/0.088=125 animals. The 95% confidence bounds for the abundance estimate were adjusted in the same way. The probability of detection on the line (g(0)) has a similar influence on abundance estimates. If the probability of detection on the line is overestimated, the proportion of the population detected will be overestimated, leading to an underestimate of density/abundance. The g(0) here is assumed to be 1.

Uncertainty in the availability estimates used was not accounted for here due to a lack of reliable published data. Should this information become available in the future, it can be directly incorporated under this modelling scheme. It should be noted that absolute abundance estimates are very sensitive to these availability adjustments. They operate as direct (inverse) multipliers, so a halving of the availability will result in a doubling of the abundance estimate. As before, g(0) adjustments would have an equivalent impact.

The following instantaneous availabilities were assumed for the species being considered:

| Species | Probability of being available to be seen at the sea surface |
|---|---|
| Minke Whale | 0.04[10] |
| White Beaked Dolphin* | 0.11[11] |
| Harbour Porpoise | 0.434[12,13] |

Table 4: Availability corrections used for the analysis. *An availability bias correction for white beaked dolphin was unavailable so a value for bottlenose dolphins was used instead.

10 1989. Joyce, G.G., Øien, N., Calambokides, J. and Cubbage, J. C. 1989. Surfacing rates of minke whales in Norwegian waters. Report of the International Whaling Commission 39, 431 – 434.

11 1995. Mate, B. R., Rossbach, K. A., Nieukirk, S. L., Wells, R. S., Irvine, A. B., Scott, M. D., and Read, A.J. Satellite-monitored movements and dive behavior of a bottlenose dolphin (*Tursiops truncatus*) in Tampa Bay, Florida. Marine Mammal Science, 11, 452-463.

12 1995. Westgate, A. J., Read, A. J., Berggren, P., Koopman, H. N., and Gaskin, D. E. Diving behaviour of harbour porpoises, *Phocoena phocoena*. Canadian Journal of Fisheries and Aquatic Sciences, 52:1064–1073.

13 2006. Thomsen, F., Laczny M. and Piper, W. A recovery of harbour porpoises (*Phocoena phocoena*) in the southern North Sea? A case study off Eastern Frisia, Germany. Helgoland Marine Research, 60(3): 189-195, doi: 10.1007/s10152-006-0021-z

# 5 MODELLING RESULTS

We present here graphical summaries of the density surface models for each of the three species. Both the graphics and associated data are provided as deliverables in conjunction with this report.

## 5.1 THE SURVEYED AREA

Notably, the spatial extent of the surveyed area differed across the survey period (Figure 7) and in particular, was much reduced in 2011 compared with 2009 and 2010. This was due to the lack of aerial survey effort in 2011. This necessarily means that any predictions based on the data falling between the green and red/black perimeters (Figure 7) when pooled across years are only supported by pre-2011 data.

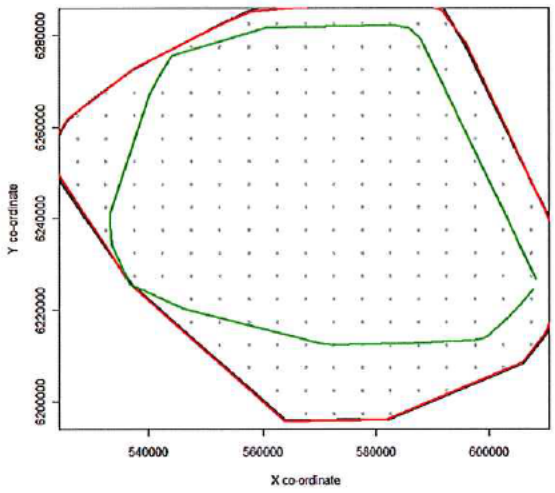


Figure 7: Visual comparison of the surveyed areas in 2009 (black line), 2010 (red line) and 2011 (green line). Notably, the surveyed area in 2011 was much reduced compared to the area surveyed area in 2009-2010 (based on The Crown Estate (TCE) aerial surveys).

All surfaces presented from this point are given in UTM, as in Figure 7, with x & y coordinates given in metres in their respective directions.

## 5.2 HARBOUR PORPOISE

### 5.2.1 Model results across the survey period (2009—2011)

The following results are fitted to data combined across the survey period and therefore only the fixed covariates (a spatial smooth and a smooth function for depth) were included in this model.

While the uncertainty surrounding the fitted spatial surface in this case meant the spatial surface was not deemed to be statistically significant under the model (Table 5), the depth relationship signaling fewer animals in shallower waters (Figure 8) was highly significant. This means for this data, the model implies the spatial structure of animal densities is explicable by bathymetry alone.

| MODEL TERM | *P*-VALUE |
|---|---|
| s(spatial surface) | 0.4576 |
| s(depth) | <0.0001 |

Table 5: GEE-based p-values for the terms in the average model.

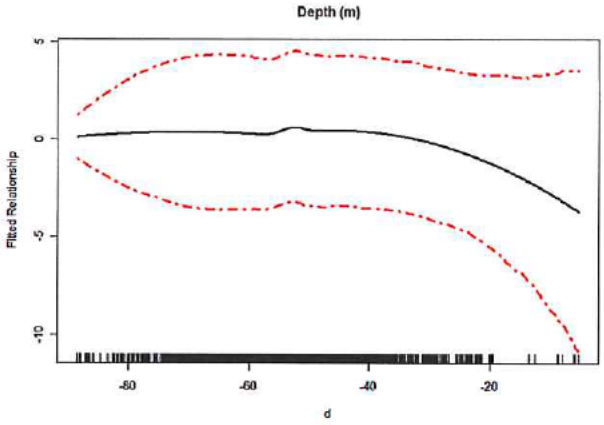


Figure 8: Estimated (link-scale) depth relationship with upper and lower GEE-based 95% confidence intervals for the model averaged over the survey period. *d*=depth.

DMP STATS The Coach House, Mount Melville House, St. Andrews, Scotland KY 168 NT, UK +44(0) 1334 477 544 mail@dmpstats.com

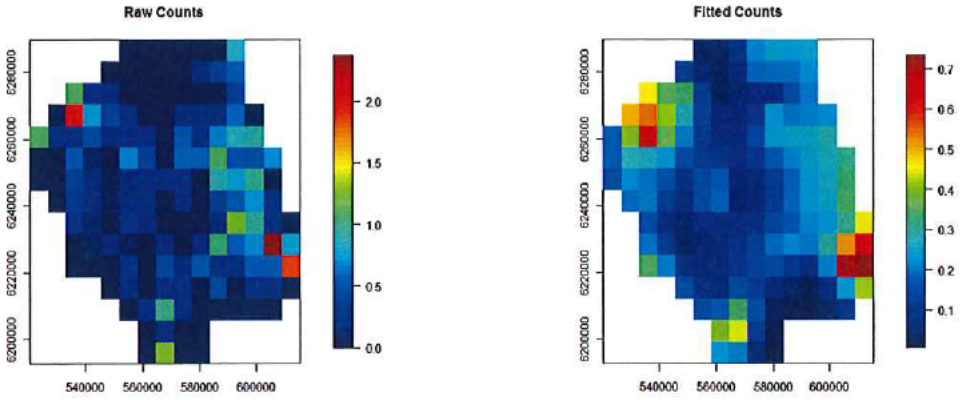


Figure 9: Left-hand plot: Raw counts averaged in each grid cell. Right- hand plot: Fitted values based on the model averaged in each grid cell. These plots are shown with the same level of resolution for comparison with the raw data. Note: the fitted values referred to here are the estimated counts per $km^2$ multiplied by the area (in $km^2$) associated with each count.

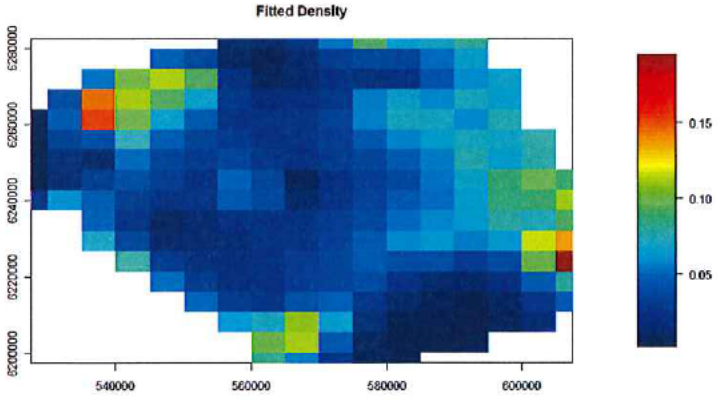


Figure 10: Estimated relative density per $km^2$ in each grid cell averaged over the survey period.

DMP STATS The Coach House, Mount Melville House, St. Andrews, Scotland KY 168 NT, UK +44(0) 1334 477 544 mail@dmpstats.com

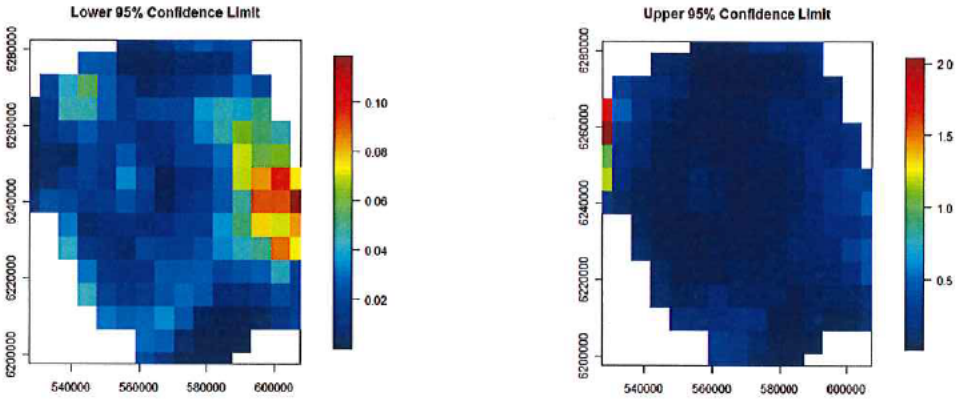


Figure 11: Upper and lower 95% confidence intervals for the relative density per $km^2$ in each grid cell averaged over the survey period.

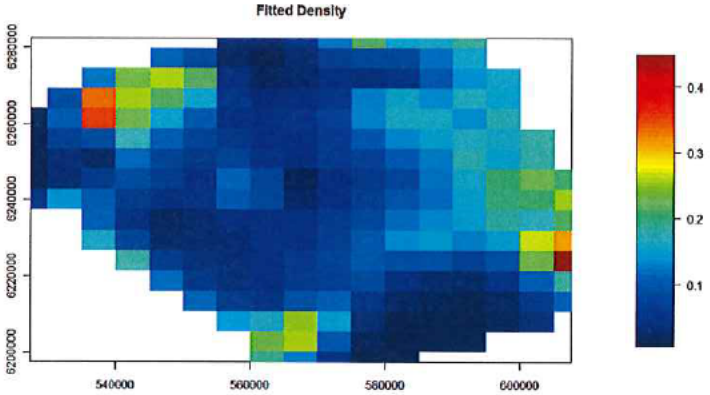


Figure 12: Estimated absolute density per $km^2$ in each grid cell averaged over the survey period, after adjusting for availability.

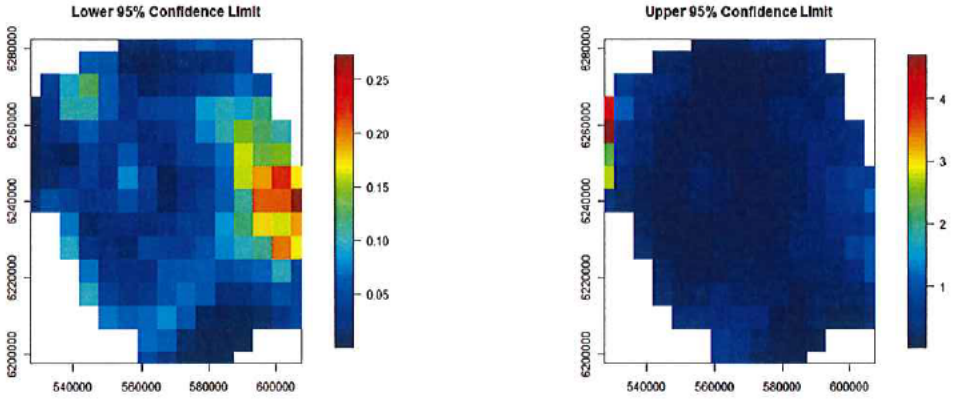


Figure 13: Upper and lower 95% confidence intervals for the absolute density per $km^2$ in each grid cell averaged over the survey period, after adjusting for availability.

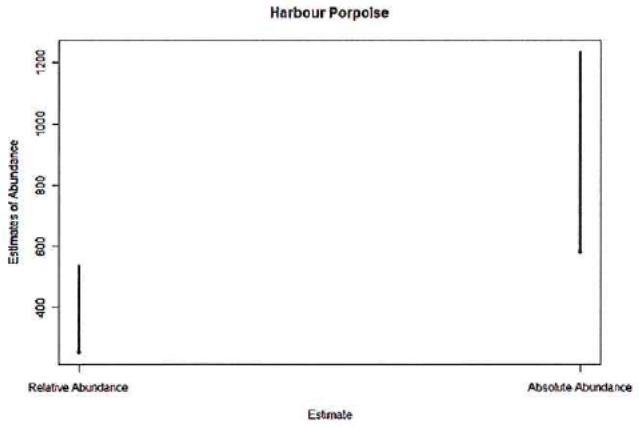


Figure 14: Average estimate of abundance across the survey area excluding and including availability adjustment with associated 95% confidence intervals.

| Abundance measure | Estimate | 95% ci |
|---|---|---|
| Relative abundance | 252.8 | (252.27, 536.02) |
| Absolute abundance | 582.4 | (581.28, 1235.07) |

Table 6: Estimates of relative and abundance for the survey area across the survey period.

### 5.2.2 Annual results

A moderately complex function, with a mix of both local and global reaching trends, was selected for harbour porpoise[14]. The spatial surface was permitted to change across years in a complex way e.g. all coefficients that define the spatial surface were permitted to vary from year to year via an interaction effect between the spatial smooth and year. Season and Year were also fitted as factor variables in the model to allow predictions to change, on average, across seasons and years.

There is a great deal of variation in the spatial distribution of harbour porpoise across the surveyed years (and a statistically significant interaction term), yet there was good agreement between the observed data for each year and the annual fitted values based on the model (Figure 17 to Figure 19).

| MODEL TERM | *P*-VALUE |
|---|---|
| **s(Depth)** | 0.2407 |
| **Survey (aerial, FoF, NnG and Inchcape)** | <0.0001 |
| **Season (Winter, Spring, Summer, Autumn)** | <0.0001 |
| **Spatial surface- Year interaction** | <0.0001 |

Table 7: GEE-basd p-values for the terms in the annual model.

Overall tests for all model terms are presented in Table 7. Notably bathymetry is not a significant predictor of animal densities (Table 7 & Figure 16), however some aspects of this may be contained within the general spatial surface. Survey type is also a highly significant predictor of average animal density, which suggests differences between surveys beyond simple differences in detection properties that were accounted for in section 3. Underlying reasons can be speculated upon, for example aerial surveys will permit some greater visibility below the surface meaning greater availability to observers. There also seems to be significant changes in average animal numbers across seasons, as indicated in Figure 15. Summer and spring are associated with an approximate 3-fold increase in harbor porpoise densities over autumn/winter. Spring & summer densities are effectively equivalent in light of uncertainties. Similarly autumn & winter are not statistically distinct.

14 (10 knots and variable $r$ across the surface).

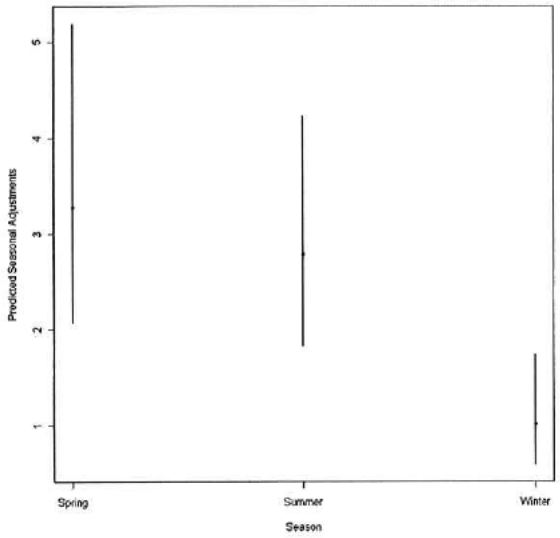


Figure 15: Estimated multiplication factors, relative to autumn, for the seasonal contributions in the model. Points indicate the estimate and vertical lines indicate the extent of the 95% confidence intervals.

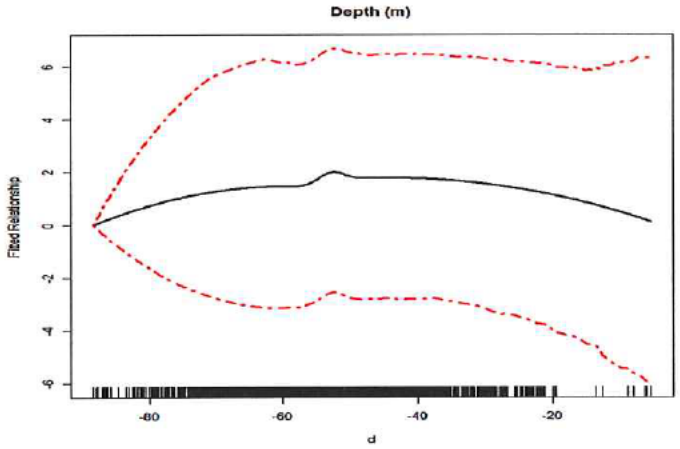


Figure 16: Estimated (link-scale) depth relationship with upper and lower GEE-based 95% confidence intervals for the model averaged over the survey period. *d*=depth.

DMP STATS The Coach House, Mount Melville House, St. Andrews, Scotland KY 168 NT, UK +44(0) 1334 477 544 mail@dmpstats.com

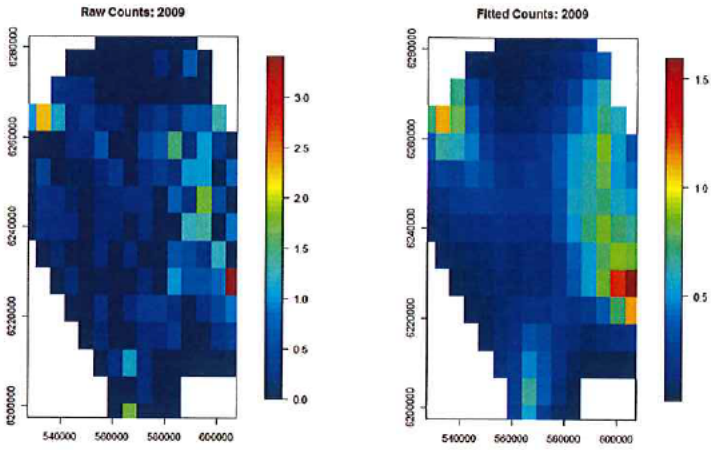


Figure 17: Left-hand plot: Raw counts in 2009 averaged in each grid cell. Right- hand plot: Fitted values based on the model for that year averaged in each grid cell. These plots are shown with the same level of resolution for comparison with the raw data. Note: the fitted values referred to here are the estimated counts per $km^2$ multiplied by the area (in $km^2$) associated with each count.

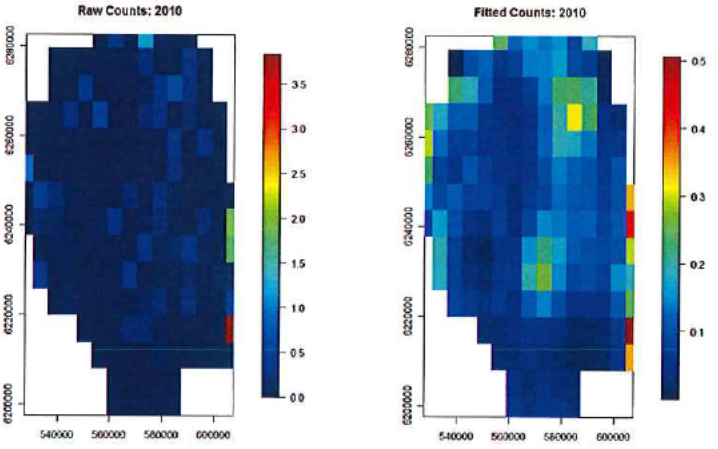


Figure 18: Left-hand plot: Raw counts in 2010 averaged in each grid cell. Right- hand plot: Fitted values based on the model for that year averaged in each grid cell. These plots are shown with the same level of resolution for comparison with the raw data. Note: the fitted values referred to here are the estimated counts per $km^2$ multiplied by the area (in $km^2$) associated with each count.

DMP STATS The Coach House, Mount Melville House, St. Andrews, Scotland KY 168 NT, UK +44(0) 1334 477 544 mail@dmpstats.com

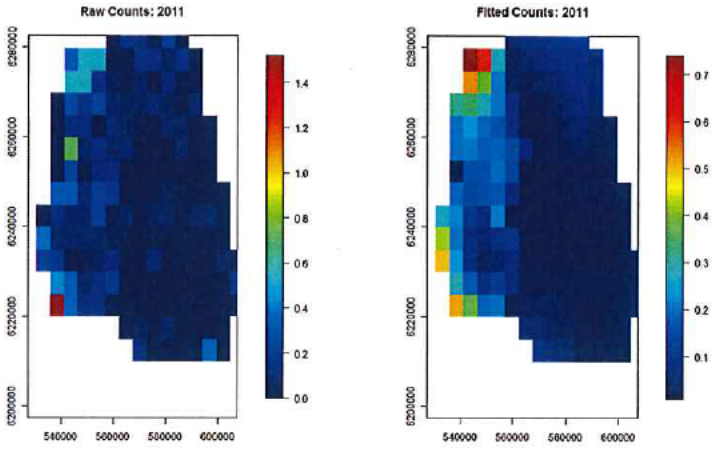


Figure 19: Left-hand plot: Raw counts in 2011 averaged in each grid cell. Right- hand plot: Fitted values) based on the model for that year averaged in each grid cell. These plots are shown with the same level of resolution for comparison with the raw data. Note: the fitted values referred to here are the estimated counts per $km^2$ multiplied by the area (in $km^2$) associated with each count.

## 5.3 WHITE BEAKED DOLPHIN

### 5.3.1 Model results across the survey period (2009—2011)

The fitted spatial surface was relatively smooth[15] but was deemed statistically significant under the model (Table 8). The depth relationship however, which signaled fewer animals in shallower waters (Figure 20), was not (Table 8). This non-significant result is likely due to the high uncertainty for the depth relationship in shallower waters where the data is sparse (Figure 20).

| MODEL TERM | *P*-VALUE |
|---|---|
| s(spatial surface) | 0.0045 |
| s(depth) | 0.6303 |

Table 8: GEE-basd p-values for the terms in the average model.

The GEE approach was justified for this model; there were statistically significant levels of positive spatio-temporal autocorrelation in model residuals. The runs test returned a test statistic of -44.1 and a p-value of <0.0001. Notably, ignoring the non-independence underestimates the *p*-values a great deal; the independence model returns p-values for both terms of <0.0001 while only the spatial surface is statistically significant under the GEE model (Table 8) once the positive autocorrelation in model residuals is accounted for.

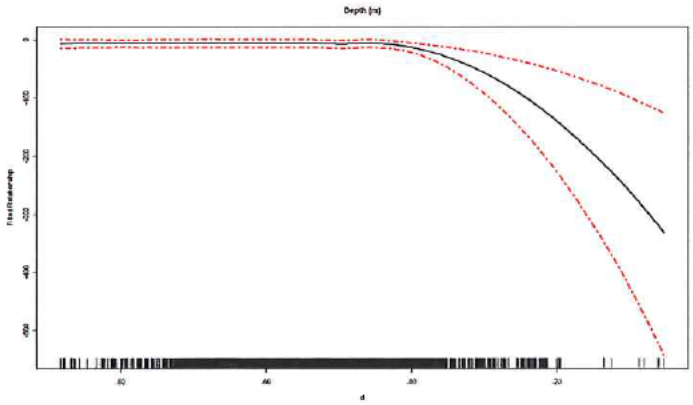

Figure 20: Estimated (link-scale) depth relationship with upper and lower GEE-based 95% confidence intervals for the model averaged over the survey period for White Beaked Dolphins.

[15] df=5 for the spatial model

DMP STATS The Coach House, Mount Melville House, St. Andrews, Scotland KY 168 NT, UK +44(0) 1334 477 544 mail@dmpstats.com

There was a hotspot identified in the north east of the survey area (Figure 21 and Figure 23), and while this area was accompanied with high uncertainty (Figure 22 and Figure 24), the lower 95% confidence bounds still identified this area as having relatively high numbers compared with other areas across the surface (Figure 22 and Figure 24). This hotspot was also evident in the raw data (Figure 25).

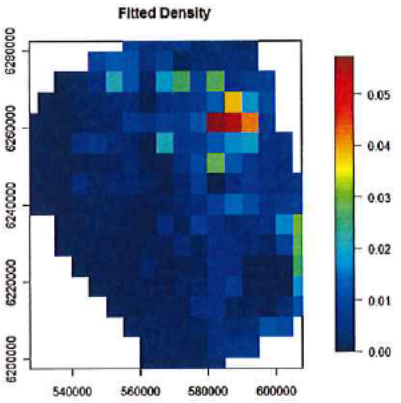


Figure 21: Estimated relative density per km$^2$ in each grid cell averaged over the survey period.

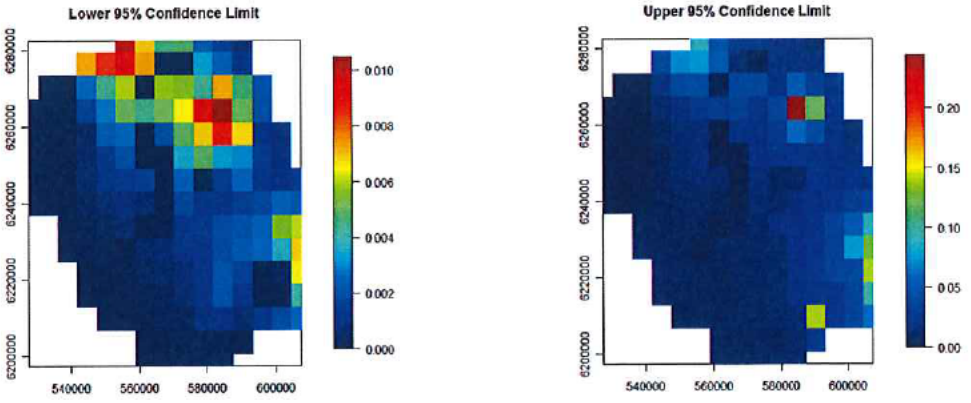


Figure 22: Upper and lower 95% confidence intervals for the relative density per km$^2$ in each grid cell averaged over the survey period.

DMP STATS The Coach House, Mount Melville House, St. Andrews, Scotland KY 168 NT, UK +44(0) 1334 477 544 mail@dmpstats.com

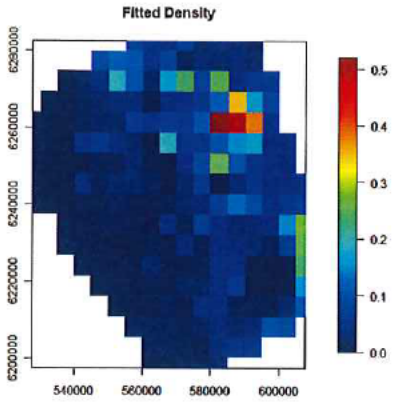


Figure 23: Estimated absolute density per $km^2$ in each grid cell averaged over the survey period, after adjusting for availability.

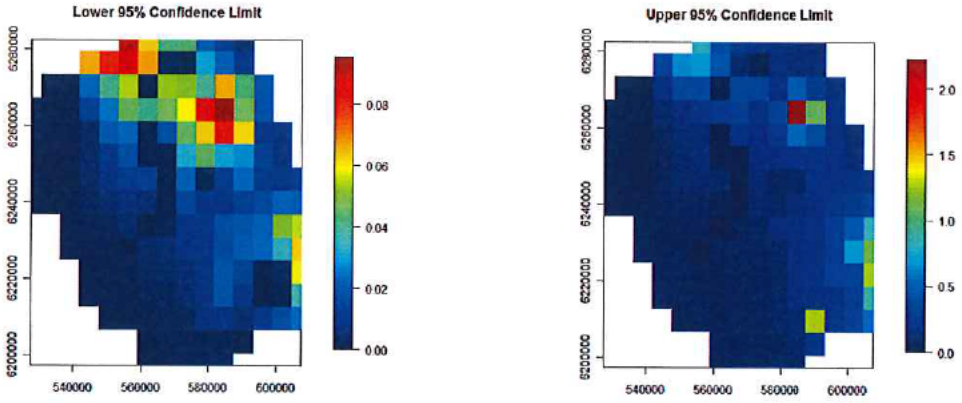


Figure 24: Upper and lower 95% confidence intervals for the absolute density per $km^2$ in each grid cell averaged over the survey period, after adjusting for availability.

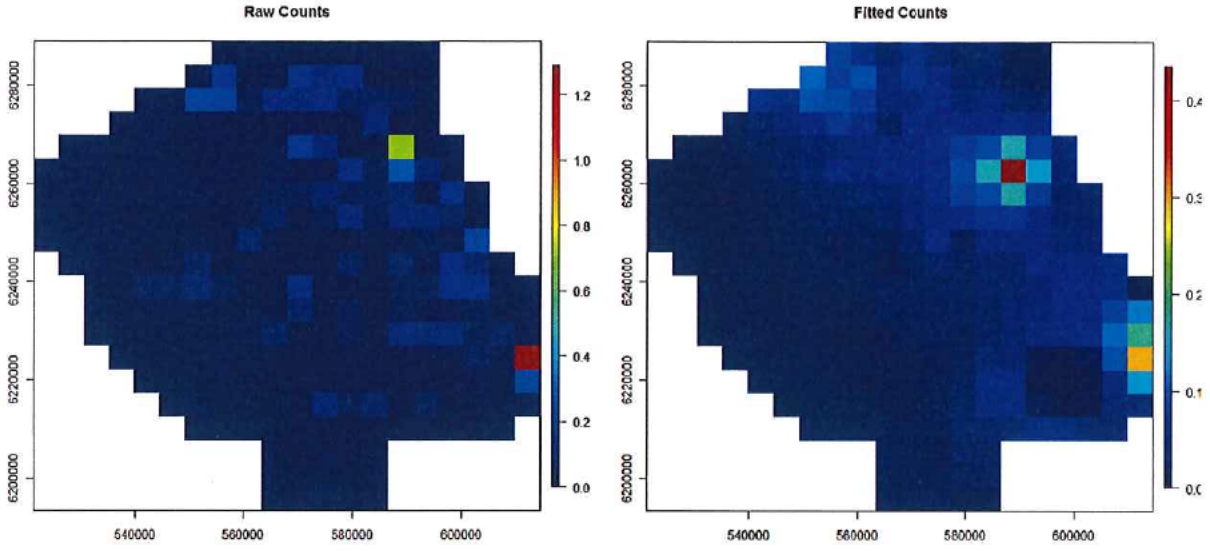


Figure 25: Comparison of the raw and fitted counts averaged over the survey period for White Beaked Dolphin.

There were very few animals estimated across the survey area, on average (approximately 32 animals; Table 9) but due to the proportion of time this species is estimated to spend underwater, this number was elevated to approximately 293 across the survey area (Table 9). There is also a great deal of uncertainty about these estimates (Table 9 and Figure 26).

| ABUNDANCE MEASURE | ESTIMATE | 95% CI |
|---|---|---|
| Relative abundance | 32.25 | (29.34, 116.09) |
| Absolute abundance | 293.18 | (266.70, 1055.37) |

Table 9: Estimates of relative and abundance for the survey area across the survey period.

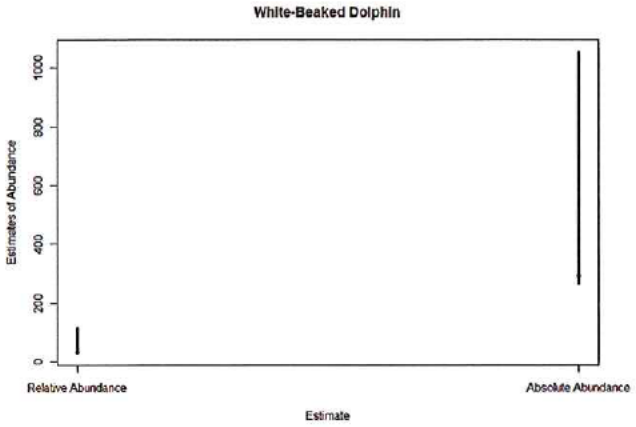


Figure 26: Average estimate of abundance across the survey area excluding and including availability adjustment with associated 95% confidence intervals.

### 5.3.2 Annual results

| MODEL TERM | *P*-VALUE |
|---|---|
| s(spatial surface) | 0.0111 |
| Year | 0.0131 |
| Survey | 0.0078 |
| s(depth) | 0.8835 |

Table 10: GEE-basd p-values for the terms in the annual models.

A smooth spatial surface was chosen for White Beaked Dolphins and while animal numbers were permitted to change annually via a factor-based variable for year (Figure 27 to Figure 32). All model terms were statistically significant in the model excepting the depth relationship (Table 10) which was also true for the model fitted to the data pooled across the survey period (Table 8).

In keeping with the model fitted to the average of the data across the survey period, the hotspot in the north east of the survey area dominates the results. Notably there is extremely high uncertainty in the South-East of the survey area, giving unrealistically high upper 95% confidence limits in this area. A GEE approach was also required for this model; there was statistically significant levels of spatio-temporal autocorrelation[16] present in model residuals which is accounted for by the model.

[16] (a runs test returned a test statistic of -62.7646, and p-value<0.00001).

### 5.3.2.1 Relative density surfaces and estimates

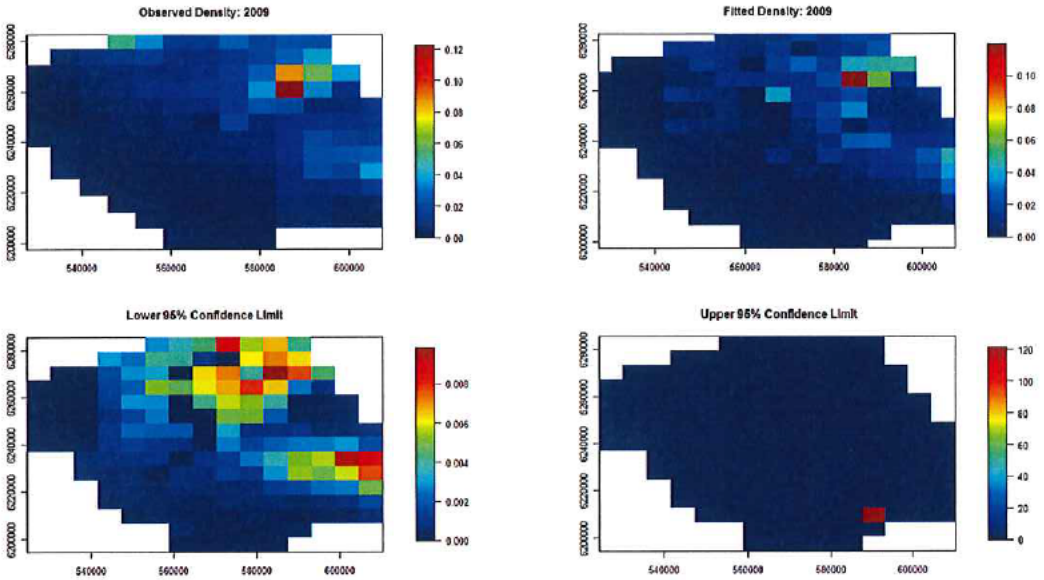


Figure 27 Estimated relative densities per km$^2$ and upper and lower 95% confidence intervals for the relative densities in 2009 averaged in each grid cell for aerial surveys (TCE).

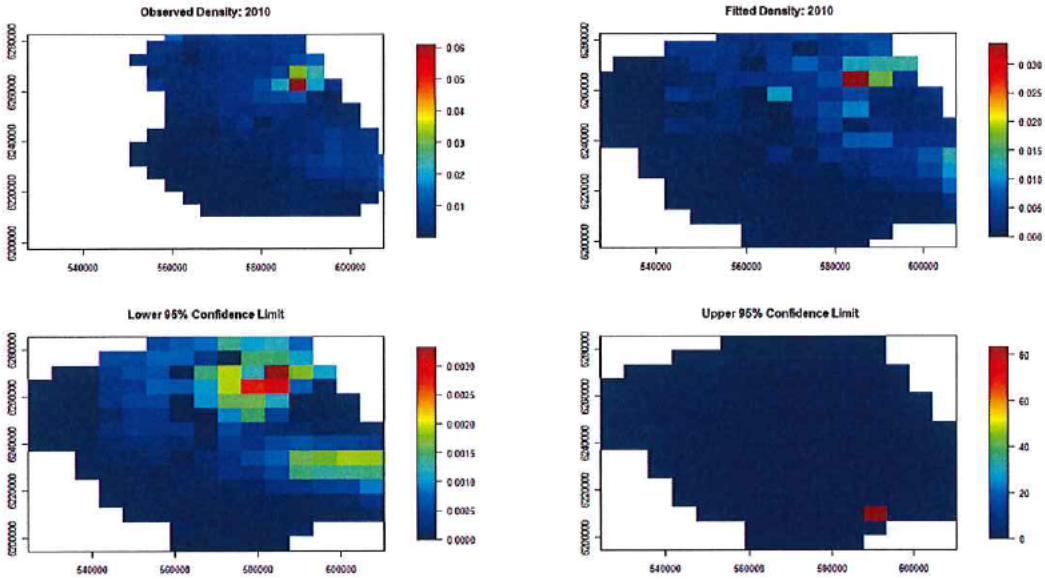


Figure 28: Estimated relative densities per km$^2$ and upper and lower 95% confidence intervals for the relative densities in 2010 averaged in each grid cell, for the Firth of Forth survey.

DMP STATS The Coach House, Mount Melville House, St. Andrews, Scotland KY 168 NT, UK +44(0) 1334 477 544 mail@dmpstats.com

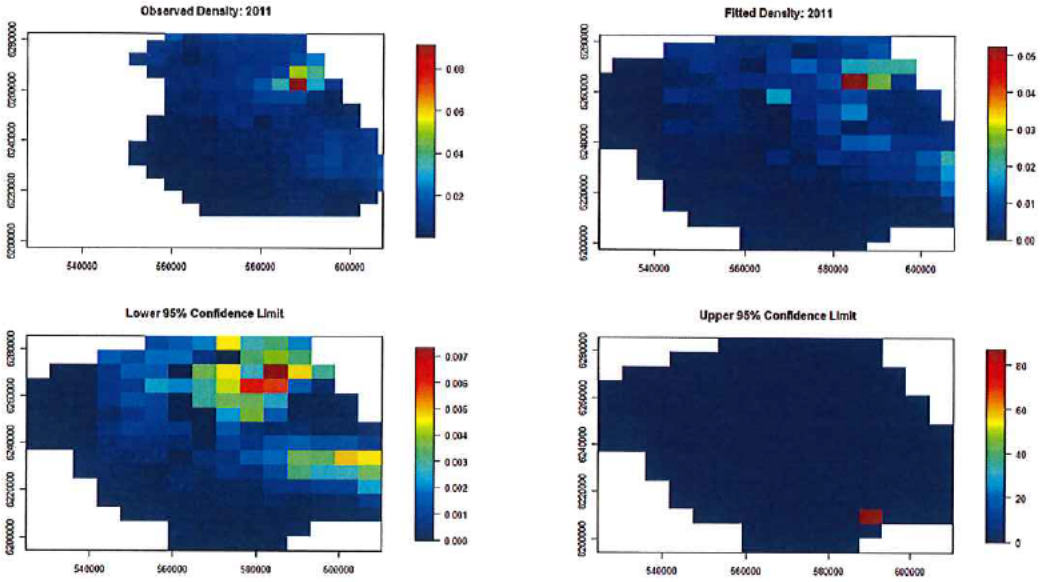


Figure 29: Estimated relative densities per km$^2$ and upper and lower 95% confidence intervals for the relative densities (on a fine grid) in 2011 averaged in each grid cell, for the Firth of Forth survey.

### 5.3.2.2 Absolute density surfaces and estimates

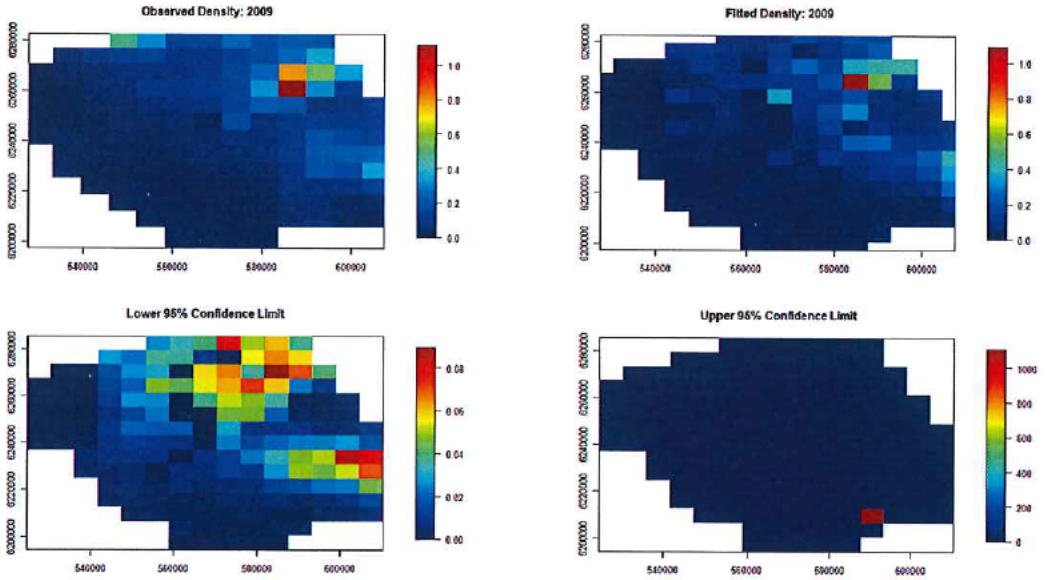


Figure 30: Estimated absolute densities per km$^2$ and upper and lower 95% confidence intervals for the absolute densities (on a fine grid) in 2009 averaged in each grid cell.

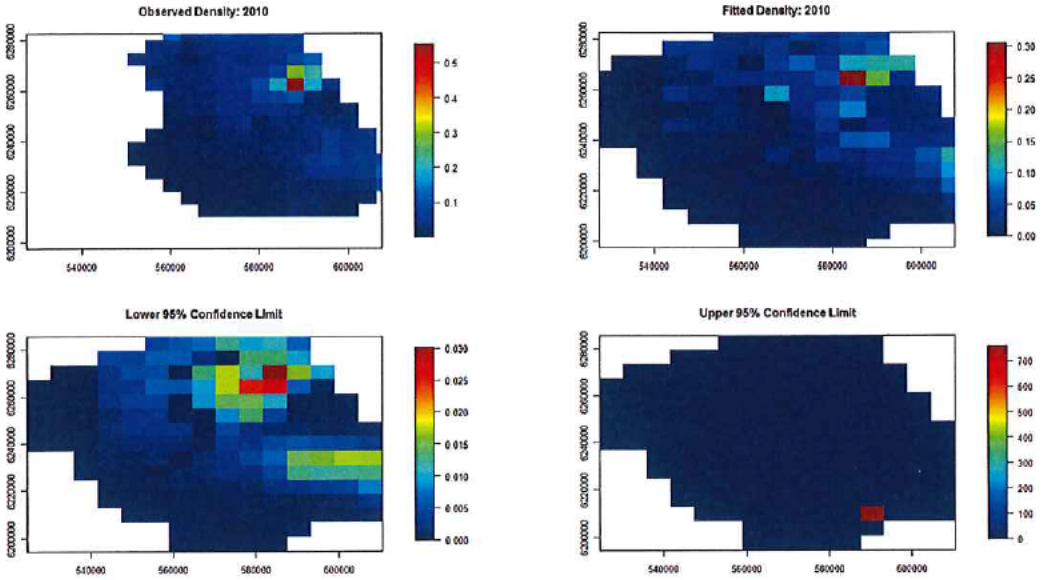


Figure 31: Estimated absolute densities per km$^2$ and upper and lower 95% confidence intervals for the absolute densities (on a fine grid) in 2010 averaged in each grid cell.

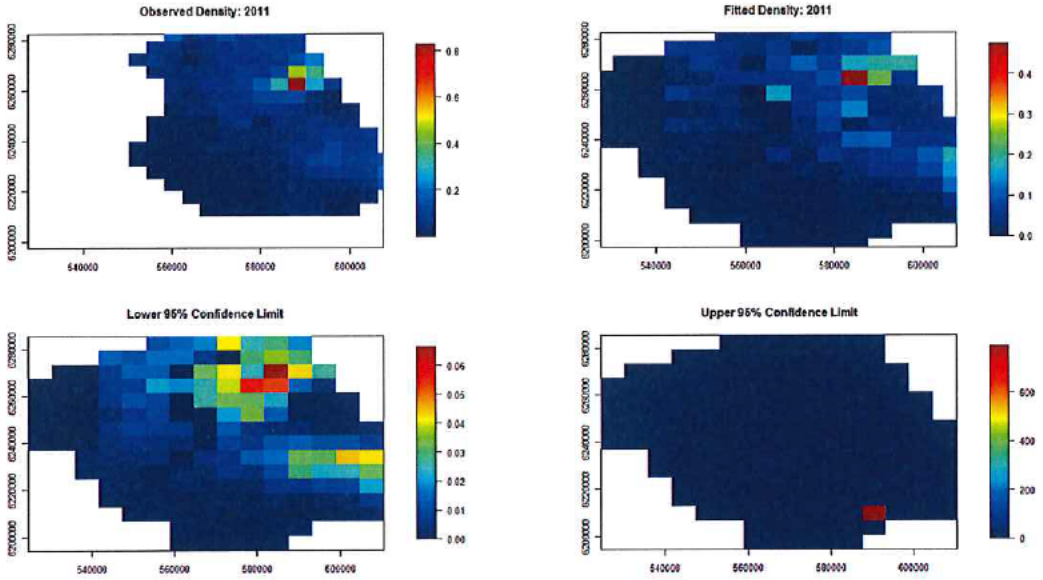


Figure 32: Estimated absolute densities per km$^2$ and upper and lower 95% confidence intervals for the absolute densities (on a fine grid) in 2011 averaged in each grid cell.

## 5.4 MINKE WHALE

### 5.4.1 Model results across the survey period (2009—2011)

The average surface for Minke Whale was chosen to be very smooth[17] and indicated higher numbers of animals in the North of the survey area, although the density was still very low in these areas in absolute terms (Figure 34). The upper and lower confidence surfaces indicate a large amount of uncertainty in the south-east corner of the survey area ranging from very low densities (close to zero) and as high as 0.4 per $km^2$ (Figure 35). The hotspots in the models correspond closely with the areas with higher counts (Figure 38).

While the spatial surface component of the model was quite smooth (and required only 4 parameters) it was relatively uncertain and only the depth relationship was statistically significant under the model (Table 11) where higher numbers of whales were seen in deeper waters (Figure 33).

| MODEL TERM | *P*-VALUE |
|---|---|
| s(spatial surface) | 0.1390 |
| s(depth) | 0.0077 |

Table 11: GEE-basd p-values for the terms in the average model.

A GEE model was required in this case; there were significant levels of positive spatio-temporal autocorrelation in model residuals[18]. Notably, both terms were statistically significant (at the 1% level) when the autocorrelation was ignored.

[17] df=4

[18] The runs test returned a test statistic of -55.08 and a *p*-value of 0.0000.

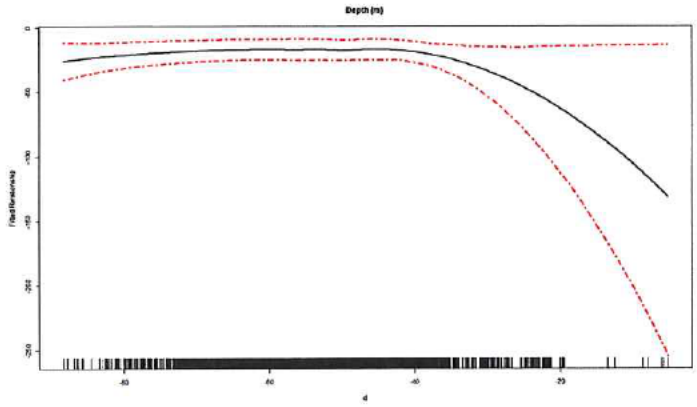


Figure 33: Estimated (Llink-scale) depth relationship with upper and lower 95% confidence intervals for the average model.

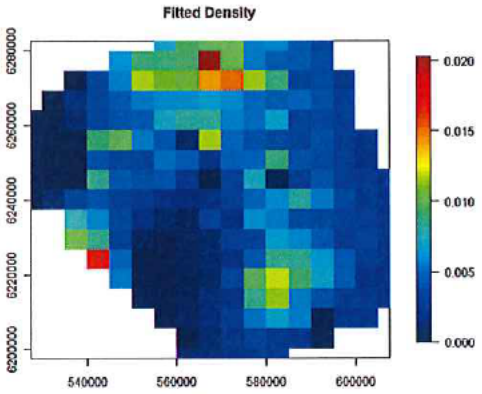


Figure 34: Estimated relative density per $km^2$ in each grid cell averaged over the survey period.

DMP STATS The Coach House, Mount Melville House, St. Andrews, Scotland KY 168 NT, UK +44(0) 1334 477 544 mail@dmpstats.com

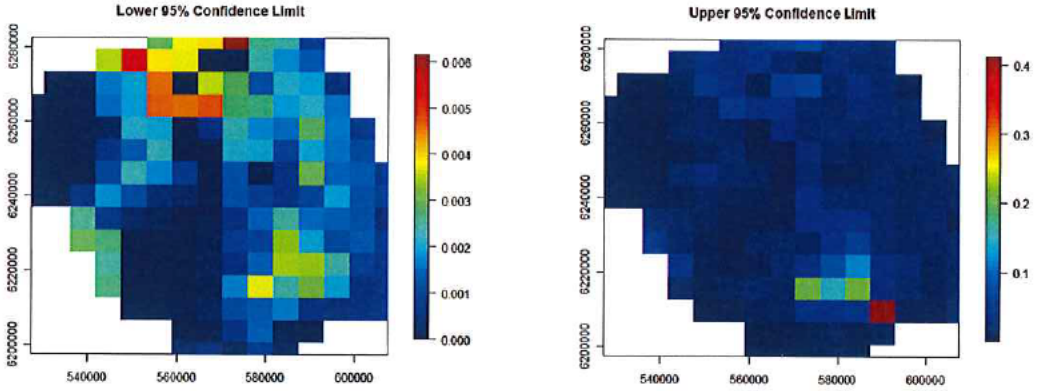


Figure 35: Upper and lower 95% confidence intervals for the relative density per $km^2$ in each grid cell averaged over the survey period.

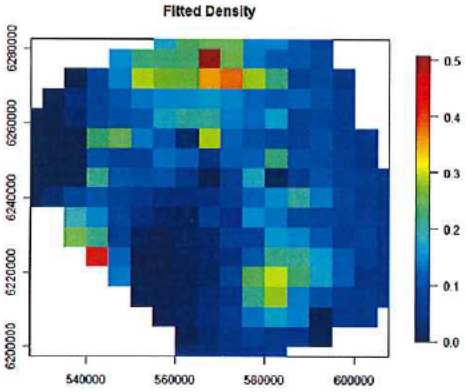


Figure 36: Estimated absolute density per $km^2$ in each grid cell averaged over the survey period, after adjusting for availability.

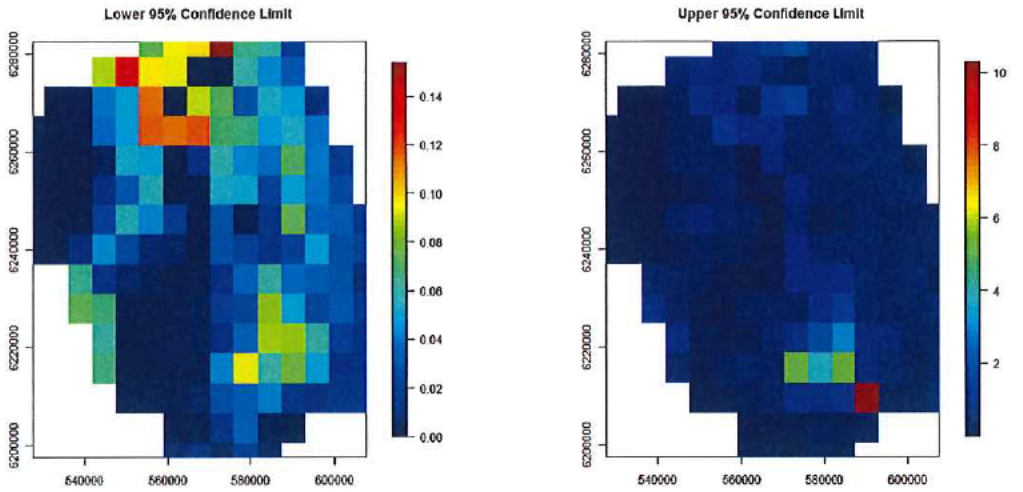


Figure 37: Upper and lower 95% confidence intervals for the absolute density per $km^2$ in each grid cell averaged over the survey period, after adjusting for availability.

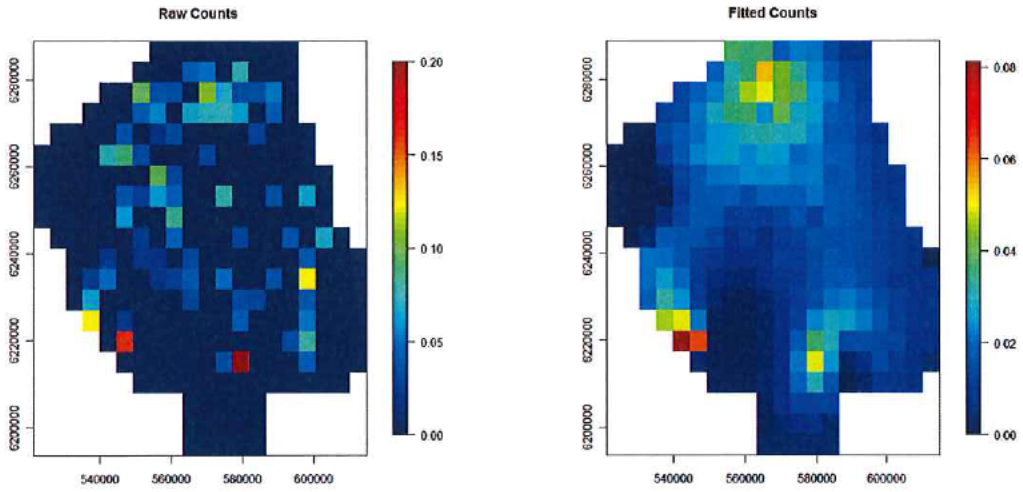


Figure 38: Comparison of the raw and fitted counts averaged over the survey period for Minke Whales.

There were very few animals estimated across the survey area, on average (approximately 24 animals; Table 12) but due to the proportion of time this species is estimated to spend underwater, this number was elevated to approximately 594 across the survey area (Table 12). There is however a huge amount of uncertainty about these estimates (Table 12 and Figure 39).

| ABUNDANCE MEASURE | ESTIMATE | 95% CI |
|---|---|---|
| Relative abundance | 23.76 | (19.31, 107.79) |
| Absolute abundance | 594.12 | (482.94, 2694.87) |

Table 12: Estimates of relative and abundance for the survey area across the survey period.

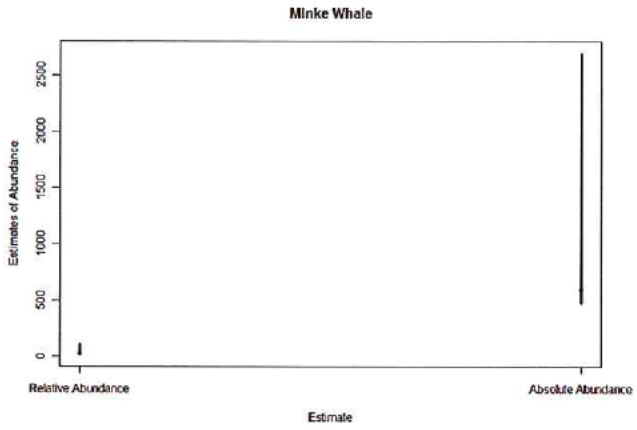


Figure 39: Average estimate of abundance across the survey area excluding and including availability adjustment with associated 95% confidence intervals.

### 5.4.2 Annual results

| MODEL TERM | *P*-VALUE |
|---|---|
| s(spatial surface) | 0.1143 |
| Year | 0.1115 |
| Survey | 0.1429 |
| s(depth) | 0.0184 |

Table 13: GEE-basd p-values for the terms in the annual models.

A relatively complicated spatial surface was chosen for Minke Whale [19] (Figure 40 to Figure 45), however none of the model terms were statistically significant excepting the depth relationship under the GEE model (Table 13). The hotspots identified in the north and south of the survey area (Figure 40 to Figure 45) are consistent with those seen in the data (Figure 38).

A GEE model was required for these data; there was significant levels of positive autocorrelation in model residuals[20] and failing to recognize this correlation resulted in *p*-values that were all too small (and statistically significant at the 5% level).

### 5.4.2.1 Relative density surfaces and estimates

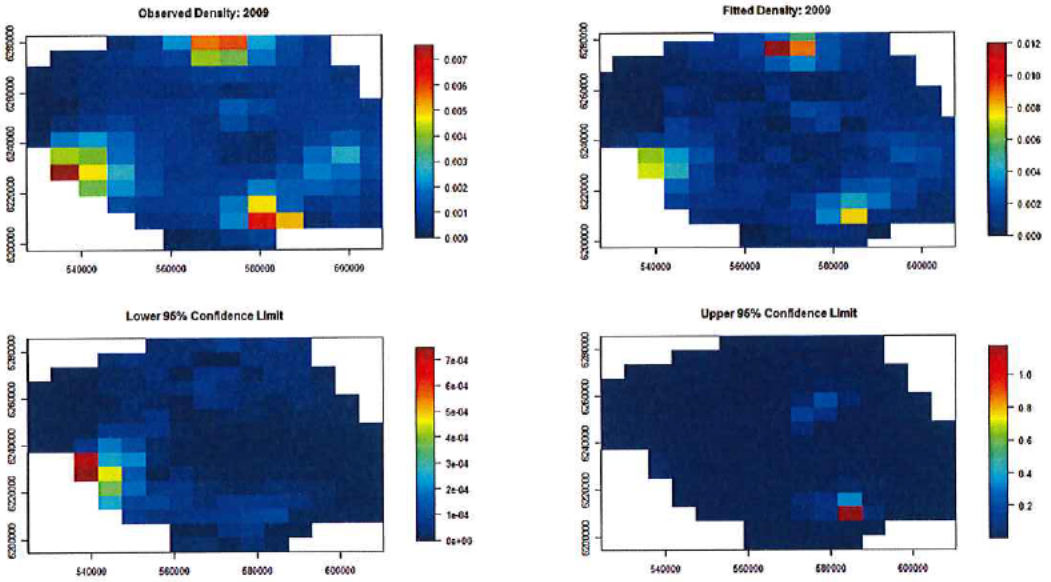


Figure 40: Estimated relative densities per km$^2$ (i.e. without adjustment for availability) and upper and lower 95% confidence intervals for the densities (on a fine grid) in 2009, averaged in each grid cell.

[19] (df=8)

[20] the runs test returned a test statistic of -84.72 and a p-value of 0.0000.

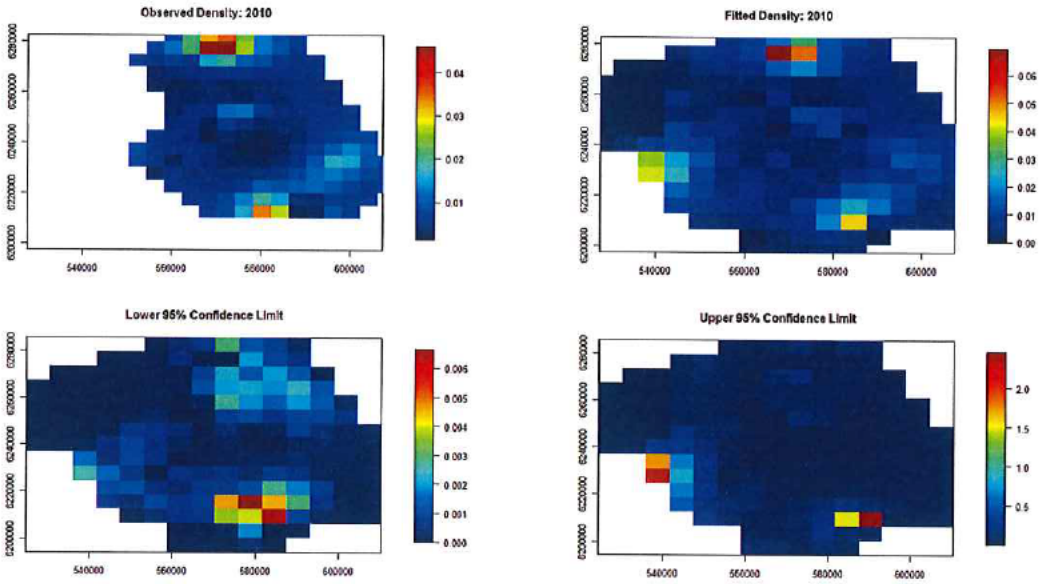


Figure 41: Estimated relative densities per km$^2$ (i.e. without adjustment for availability) and upper and lower 95% confidence intervals for the densities (on a fine grid) in 2010 averaged in each grid cell.

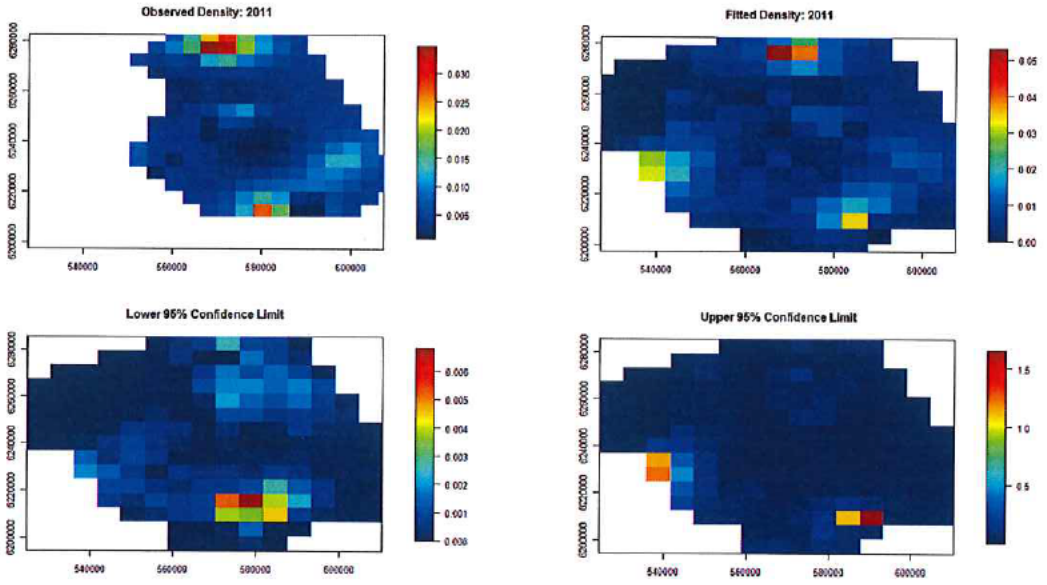


Figure 42: Estimated relative densities per km$^2$ (i.e. without adjustment for availability) and upper and lower 95% confidence intervals for the densities (on a fine grid) in 2011 averaged in each grid cell.

### 5.4.2.2 Absolute density surfaces and estimates

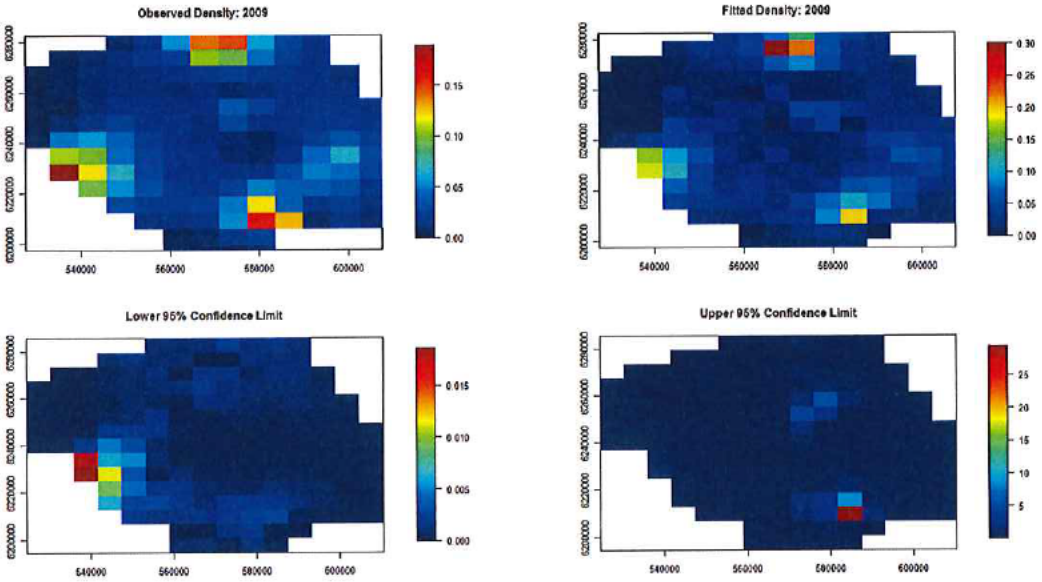


Figure 43: Estimated absolute densities per km$^2$ (i.e. with adjustment for availability) and upper and lower 95% confidence intervals for the densities (on a fine grid) in 2009 averaged in each grid cell.

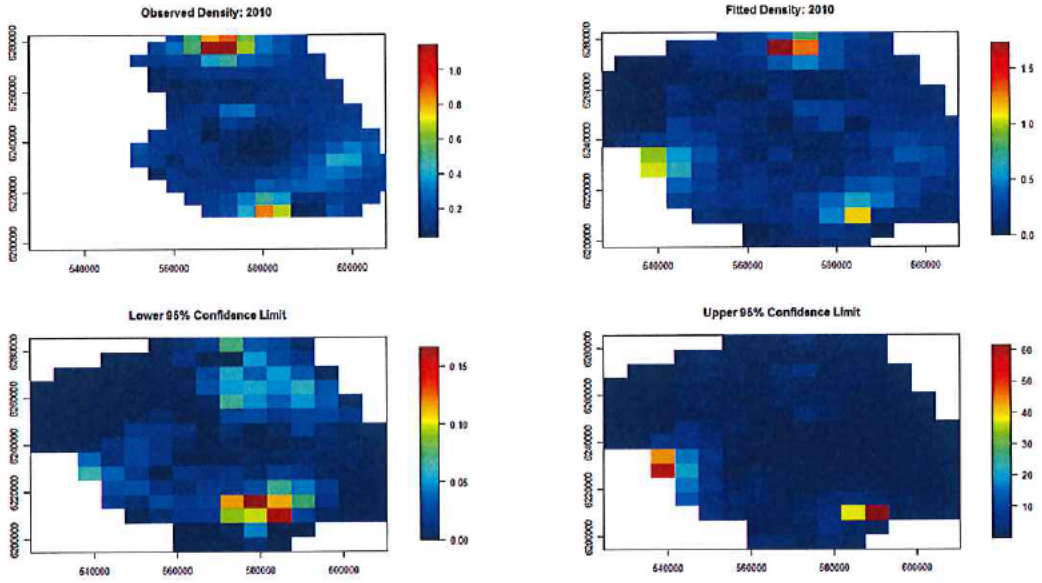


Figure 44: Estimated absolute densities per km$^2$ (i.e. with adjustment for availability) and upper and lower 95% confidence intervals for the densities (on a fine grid) in 2010 averaged in each grid cell.

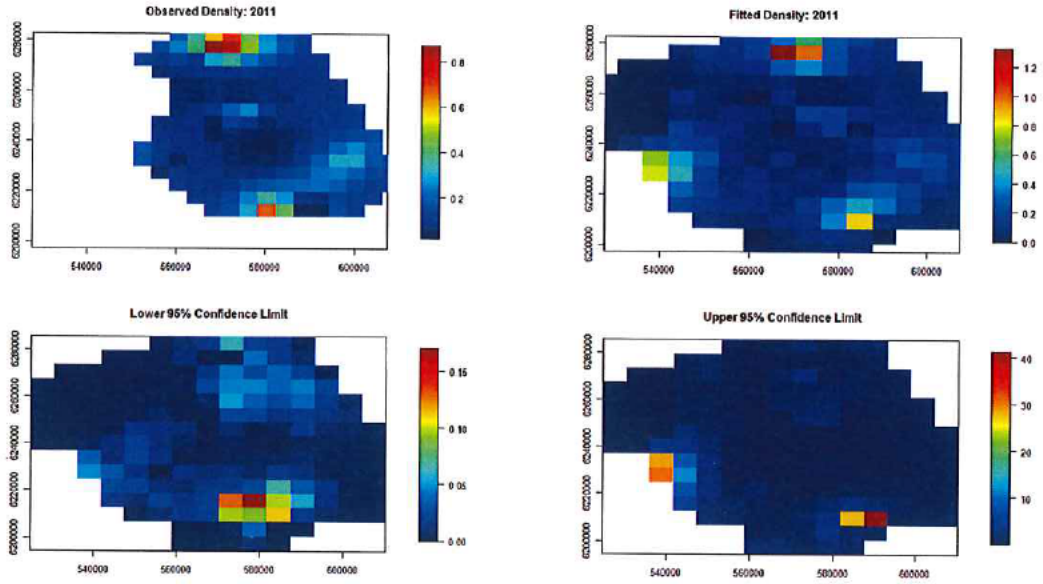


Figure 45: Estimated absolute densities per km$^2$ (i.e. with adjustment for availability) and upper and lower 95% confidence intervals for the densities (on a fine grid) in 2011 averaged in each grid cell.

DMP STATS The Coach House, Mount Melville House, St. Andrews, Scotland KY 168 NT, UK +44(0) 1334 477 544 mail@dmpstats.com

## 6 MODEL COMPARISON AND VALIDATION

The spatially adaptive model results for harbour porpoise, minke whale and white-beaked dolphin contained within this report were compared with Generalized Additive Modelling (GAM) results with smoothness across the surface chosen, as is customary, using MGCV[21]. Using cross-validation as the independent measure (described in section 4.3), the GAMs performed worse than the spatially adaptive models selected here in all cases (Table 14).

| SPECIES | GAM CV | SPATIALLY ADAPTIVE GAM/GEE CV SCORE |
|---|---|---|
| Minke Whale | 325.9 | 321.5 |
| White Beaked Dolphin | 828.3 | 822.0 |
| Harbour Porpoise | 4699.1 | 4557.3 |

Table 14: CV scores for the GAMs and the spatially adaptive GAMs/GEEs fitted in this report.

While some of these CV scores between the spatially adaptive models and the GAM-based CV scores appear close, the GAM-based CV scores were worse than all spatially adaptive models trialled for selection (regardless of complexity) for Harbour porpoise. The GAMs also performed worse for 67% of the candidate models considered for selection (including the selected model) for White Beaked dolphin. The GAM-based CV score was also worse for 78% of the candidate models considered for selection for Minke Whale.

The spatial surfaces produced by the GAMs are compared for each species separately with the spatially adaptive model surfaces produced here; the spatially adaptive models in this report produced both more smooth and more flexible surfaces when compared with the off-the-shelf GAM results (Sections 6.1, 6.2 and 6.3).

[21] **2011**. Wood, S.N. Fast stable restricted maximum likelihood and marginal likelihood estimation of semiparametric generalized linear models. Journal of the Royal Statistical Society (B) 73(1):3-36

## 6.1 HARBOUR PORPOISE

The two approaches produce similar surfaces in 2011 but differ more markedly in 2009 and 2010 (Figure 46 and Figure 47). In contrast, the GAMs concentrate the animals on the east and west of the survey area in 2010 and 2011 respectively, while the spatially adaptive models indicate a more localised distribution across the area in 2010 and 2011 (Figure 46 and Figure 47). This difference in distribution is supported by the cross validation results (Table 14).

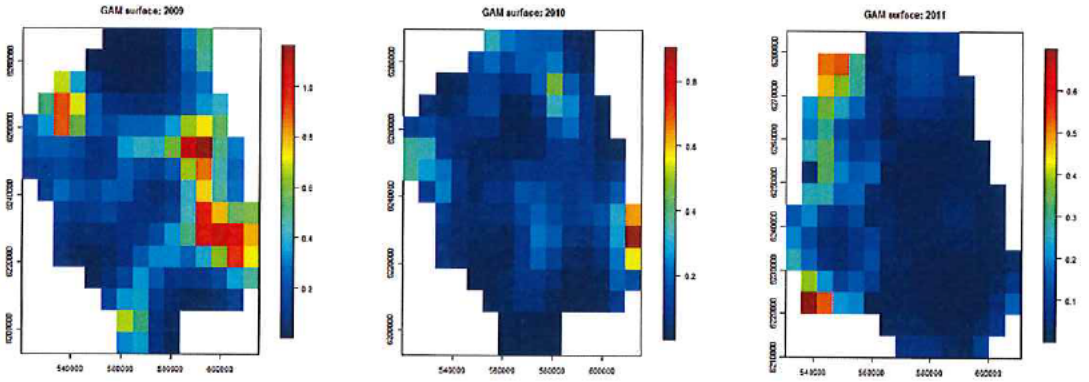


Figure 46: Estimated densities per km$^2$ (without adjustment for availability) based on an MGCV-based GAM for the Harbour Porpoise data.

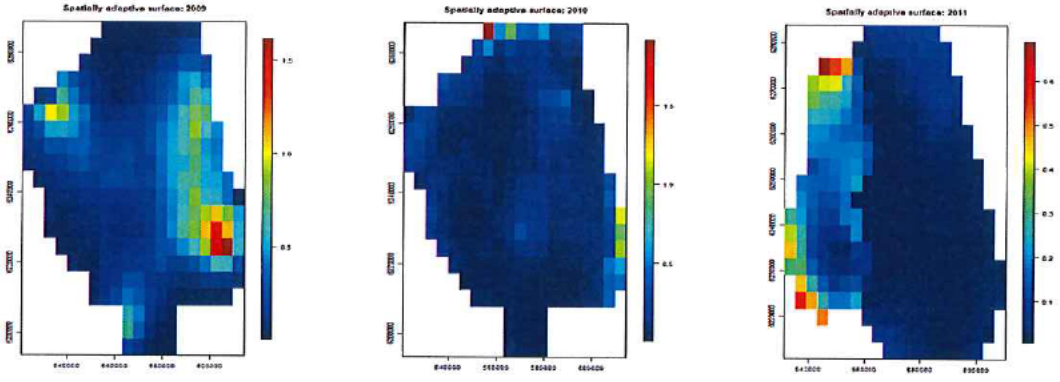


Figure 47: Estimated densities per km$^2$ (without adjustment for availability) based on the selected spatially adaptive model for the Harbour Porpoise data.

## 6.2 MINKE WHALE

While the granularity of the prediction grid is relatively coarse, differences apparent between the GAM surfaces and the spatially adaptive surfaces. In particular, hotspots are more localised in the models chosen here (Figure 48 and Figure 49). The off-the-shelf GAMs are much smoother and predict less change from year to year, despite also being permitted an interaction term with year (as was fitted in the chosen models here). Notably, under the GAM the numbers are consistently higher in the North of the surveyed area and this was predicted to persist in all three years (Figure 48).

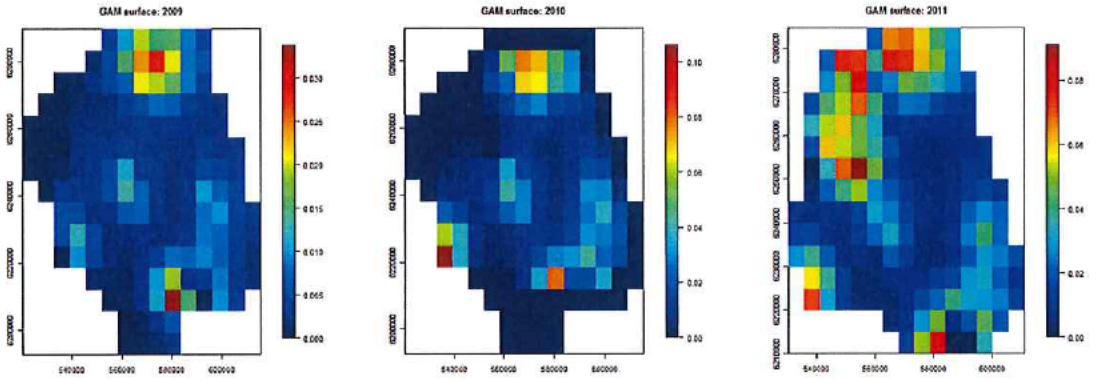


Figure 48: Estimated densities per km$^2$ (without adjustment for availability) based on an MGCV-based GAM for the Minke Whale data.

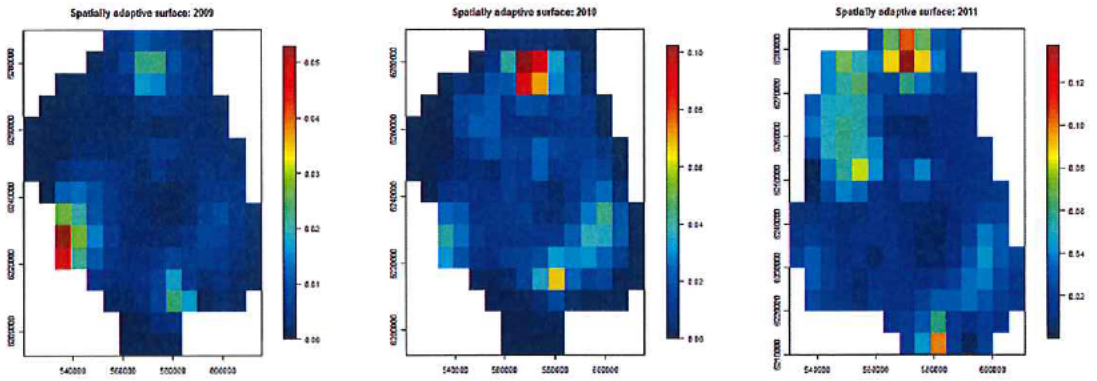


Figure 49: Estimated densities per km$^2$ (without adjustment for availability) based on the selected spatially adaptive model for the Minke Whale data.

## 6.3 WHITE BEAKED DOLPHIN

As seen for Minke Whale, the hotspots in the spatially adaptive models fitted here are more concentrated/localized for White-beaked dolphin (Figure 50 and Figure 51). The GAMs are much smoother for all years (Figure 50). The cross validation exercise suggests that this extra local behaviour is however more appropriate, even for data unseen by the model.

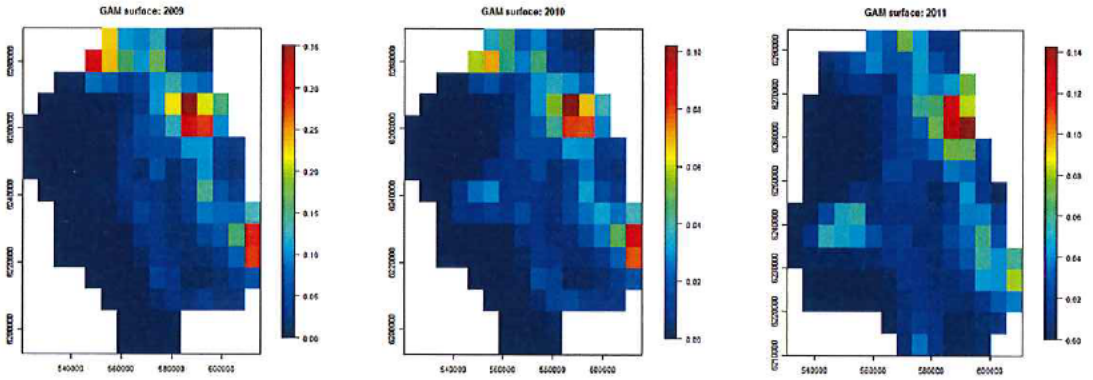


Figure 50: Estimated densities per km$^2$ (without availability adjustment) from a MGCV-based GAM for the White-Beaked dolphin data.

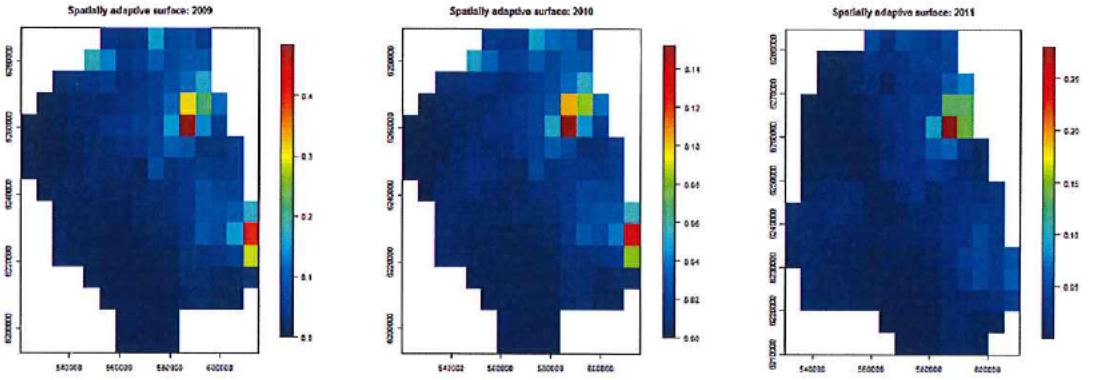


Figure 51: Estimated densities per km$^2$ (without adjustment for availability) based on the selected spatially adaptive model for the White-Beaked dolphin data.

DMP STATS The Coach House, Mount Melville House, St Andrews, Scotland KY 168 NT, UK +44(0) 1334 477 544 mail@dmpstats.com

## 7 CONCLUDING REMARKS

This document and associated data-files constitute fulfillment of analysis requirements for the Forth and Tay Offshore Wind Developers Group Cetacean Survey Data Analysis (to 2011). The tasks and outputs are summarized here:

- Preliminary data cleaning and treatment to provide dataset amenable to statistical analysis.
- Analyses to account for decreasing detection probability with distance from observation platform (via Distance Sampling) found in §3.
- Production of species density maps for 3 species: White-beaked dolphins, minke whales & harbour porpoise. A number of variants are provided (§5):
  - Relative estimates based on analysis of the detected animals.
  - Absolute abundance surfaces by adjusting these relative surfaces to account for availability bias (§4.4).
  - Surfaces averaged over the survey period.
  - Surfaces at a seasonal level for species that supported that resolution. This was only possible for harbour porpoises. The data for these are provided in their entirety in the deliverable datasets, a summary is given in Figure 15.
  - Empirical upper and lower 95% confidence surfaces for each density surface from bootstrapping.
- Detailed technical notes regarding the surface modeling methodologies §4
- The data files underpinning all these surfaces are available in CSV format, selections of which have been provided to SMRU Ltd.